



OPEN ACCESS

EDITED BY

Thiago Pereira Santos,
Fluminense Federal University, Brazil

REVIEWED BY

Fabienne Marret,
University of Liverpool, United Kingdom
Lucilla Capotondi,
National Research Council (CNR), Italy

*CORRESPONDENCE

Janne Repschläger
✉ j.repschlaeger@mpic.de

RECEIVED 28 February 2023

ACCEPTED 03 April 2023

PUBLISHED 24 April 2023

CITATION

Repschläger J, Weinelt M, Schneider R,
Blanz T, Leduc G, Schiebel R and Haug GH
(2023) Disentangling multiproxy temperature
reconstructions from the subtropical North
Atlantic.

Front. Ecol. Evol. 11:1176278.

doi: 10.3389/fevo.2023.1176278

COPYRIGHT

© 2023 Repschläger, Weinelt, Schneider, Blanz,
Leduc, Schiebel and Haug. This is an
open-access article distributed under the terms
of the [Creative Commons Attribution License
\(CC BY\)](#). The use, distribution or reproduction
in other forums is permitted, provided the
original author(s) and the copyright owner(s)
are credited and that the original publication in
this journal is cited, in accordance with
accepted academic practice. No use,
distribution or reproduction is permitted which
does not comply with these terms.

Disentangling multiproxy temperature reconstructions from the subtropical North Atlantic

Janne Repschläger^{1*}, Mara Weinelt², Ralph Schneider³,
Thomas Blanz³, Guillaume Leduc⁴, Ralf Schiebel¹ and
Gerald H. Haug^{1,5}

¹Climate Geochemistry Department, Max Planck Institute for Chemistry, Mainz, Germany,

²Paleoclimatology, Institute of Prehistoric and Protohistoric Archaeology, University of Kiel, Kiel,

Germany, ³Paleoceanography, Institute of Geosciences, Kiel University, Kiel, Germany, ⁴Centre
Européen de Recherche et d'Enseignement des Géosciences de l'Environnement (CEREGE), Aix-
Marseille Université, French National Centre for Scientific Research (CNRS), French National Institute for
Sustainable Development (IRD), French National Research Institute for Agriculture, Food and
Environment (INRAE), Collège de France, Aix-en-Provence, France, ⁵Department of Earth Sciences, ETH
Zurich, Zurich, Switzerland

Reliable reconstruction of past sea surface temperature (SST) is of prime importance for understanding the Earth's sensitivity to external forcing. Yet, it remains a major challenge in paleoceanography because comparison between SST estimates from different proxies reveals mismatches and raise the question as to what the contrasting proxies actually record. A better understanding of these mismatches in the light of seasonal occurrence of the proxy bearing organisms (archives) and water mass changes help to assess climate models. Here, we analyze data from the last deglaciation using a sediment core site situated at the northern boundary of the North Atlantic subtropical gyre influenced by fast latitudinal migrations of the subtropical Azores Front (AF) and resulting changes in water masses that may affect the SST records. Differences between the SST estimates from different deglacial SST reconstructions obtained from (1) Mg/Ca in planktic foraminifer tests, (2) alkenone $U^{K'}_{37}$, and (3) planktic foraminifer assemblages (SIMMAX), are assumed to result from the ecology of the proxy bearing organisms, and are assessed for the impact on different SST reconstructions from local seawater $\delta^{18}\text{O}$ ($\delta^{18}\text{O}_w$) reconstructions. The general trends of SSTs from all four proxies confirm the well-known deglacial succession of warm and cold events. Mismatches between amplitudes of temperature changes are explained by differences in the phenology of the proxy-bearing organisms and local changes in hydrography. The combination of $\delta^{18}\text{O}$ SST from the three different archives of $\delta^{18}\text{O}_w$ reconstructions may cause offsets that exceed the climate driven signals.

KEYWORDS

sea surface temperature, multiproxy, deglacial, subtropical, North Atlantic, seasonality, planktic foraminifera fauna analyses

1. Introduction

Many different sea surface temperature (SST) reconstructions based on microfossils and geochemical methods exist for the global ocean, and on time scales from millennia to millions of years. SST reconstructions derived from different proxies that are extracted from the same sediment sample reveal mismatches (e.g., Chapman et al., 1996; Steinke et al., 2008; Jansen et al., 2009; Leduc et al., 2010, 2017; Schneider et al., 2010; Sicre et al., 2013). These differences become evident by comparing, for example, results of the CLIMAP Project Members (1981) and MARGO Project Members (2009) projects that have provided global maps of temperature estimates based on various proxies for the Last Glacial Maximum. While CLIMAP Project Members (1981) reconstructed a glacial warming of the subtropical regions using a combination of different transfer functions, the results of the MARGO Project Members (2009) multiproxy approach may indicate a slight glacial cooling of 2°C for the same region. In addition, multiproxy compilations (Annan and Hargreaves, 2013; Osman et al., 2021) combined with data assimilation partially differ from the MARGO Project Members (2009) dataset.

It is generally argued that discrepancies between different proxy reconstructions are caused by the unique nature of these archives, i.e., the specific ecology of any signal-bearing organism that may be affected by SST changes to different degrees (Jonkers et al., 2010, 2013; Leduc et al., 2010; Schneider et al., 2010; Lohmann et al., 2012; Sicre et al., 2013; Telford et al., 2013; Hessler et al., 2014). Ecological changes may include the seasonal occurrence and varying preferences in dwelling depths of the signal-bearing organisms that are influenced by various oceanographic factors such as vertical and horizontal differences of water mass boundaries, salinity changes, sea ice extent, as well as changes in nutrient availability (Pérez-Folgado et al., 2003; Kisakürek et al., 2008; Storz et al., 2009; Jonkers et al., 2010, 2013; Leduc et al., 2010, 2014; Schneider et al., 2010; Sabbatini et al., 2011; Lohmann et al., 2012; Sicre et al., 2013; Telford et al., 2013; Kretschmer et al., 2016). The effect of variations of these environmental parameters on the marine biota may have a larger effect on the proxy than the temperature change itself (Huybers and Curry, 2006). Thereby, the assumption of a constant relationship between the temperature of ambient seawater and the temperature in given proxy records may be violated (Telford et al., 2013; Laepple and Huybers, 2014).

The discrepancies between SST proxies have been regarded as weaknesses of one or the other method (see summary in MARGO Project Members, 2009). However, careful consideration of ecological differences of the organisms such as planktic foraminifers and coccolithophores may help to understand mismatches between the SST reconstructions. In this study, we reinvestigate a multiproxy temperature dataset, consisting (1) of published, geochemical (Mg/Ca) data from three different planktic foraminifer species (Repschläger et al., 2015, 2017), and (2) $U^{K'}_{37}$ temperature reconstructions (Schwab et al., 2012) with (3) published (Weinelt et al., 2015) and new data of faunal assemblages at centennial resolution, and new microfossil based SIMMAX SST reconstructions from the subtropical North Atlantic covering the last 15.5 ka BP. Data are from sediment core GEOFAR KF16/MD08-3180 southeast of the Azores Islands, located at the

northern boundary of the subtropical gyre (Figure 1). The coring site is situated between temperate mesotrophic subpolar waters to the north and warmer oligotrophic subtropical waters to the south of the Azores Front (AF).

Phytoplankton production in the North Atlantic increases in spring at low latitudes and successively migrates northward with rising temperatures until late summer (e.g., Henson et al., 2009; Schiebel et al., 2011). Once surface ocean mixing deepens the mixed layer in autumn, biological production increases and a second less pronounced phytoplankton bloom may form (Schiebel et al., 2001). The strength, timing, and location of phytoplankton production in Azores waters is highly sensitive to changes in the strength of the North Atlantic oscillation (NAO) (Henson et al., 2009). Spring phytoplankton production starts earlier during negative than during positive NAO phases. This strong coupling of the phytoplankton bloom to the NAO indicates the strong coupling between the AF region and the North Atlantic climate on short timescales. On longer timescales, the Azores Front Current System is assumed to affect the stability of Atlantic Meridional Overturning Circulation (AMOC) as it acts as a potential reservoir for heat during glacial and deglacial weak phases of the AMOC (e.g., Repschläger et al., 2015, 2017).

On glacial to interglacial time scales, the position of the AF is thought to have changed latitude (Schiebel et al., 2002a). Other records from the Azores coring site indicate surface water cooling and southward movement of the AF during cold Heinrich event 1 (H1) and Younger Dryas, YD (Schwab et al., 2012; Repschläger et al., 2015). A relatively low amplitude in the $U^{K'}_{37}$ temperature record compared to the Iberian Margin is observed for the deglacial period and explained with a shift of the main alkenone production from spring to summer (Schwab et al., 2012) during cold periods. Surface and subsurface temperature reconstructions from different foraminifer species have been explained by heat storage in subsurface waters (Repschläger et al., 2015, 2017). These results indicate that the ecology of the different proxy bearing organisms at the coring site affects the observed temperature signal.

In the following,

(1) We test the behavior of different temperature proxies over the last deglaciation under consideration of archive-specific differences in ecology. To better explain the discrepancies between individual SST reconstructions, and to gain better insight into the deglacial and Holocene changes in surface hydrology of the Azores Current (AC) with respect to (a) seasonal temperature changes, (b) surface ocean stratification, and (c) water mass changes.

(2) We assess the plausibility of the SST reconstructions comparing our SST with published SST reconstructions (Obbink et al., 2010; Thornalley et al., 2010, 2011; Repschläger et al., 2015) and fresh water-forced simulation (i.e., salinity) experiments.

(3) To assess local salinity changes, classically, ice volume and temperature effects are subtracted from stable oxygen isotope measurements performed on surface-dwelling foraminifers (e.g., Shackleton, 1974; Duplessy et al., 1991; Waelbroeck et al., 2002). For this purpose, temperature reconstructions from Mg/Ca, $U^{K'}_{37}$, and SIMMAX are used and combined with the $\delta^{18}O$ signal of surface and subsurface dwelling planktic foraminifer species of varying phenology (Schiebel and Hemleben, 2000). Under the assumption that the different temperature reconstructions are potentially reflecting different seasons and water depths, the combination of temperature and $\delta^{18}O$ values from different proxy

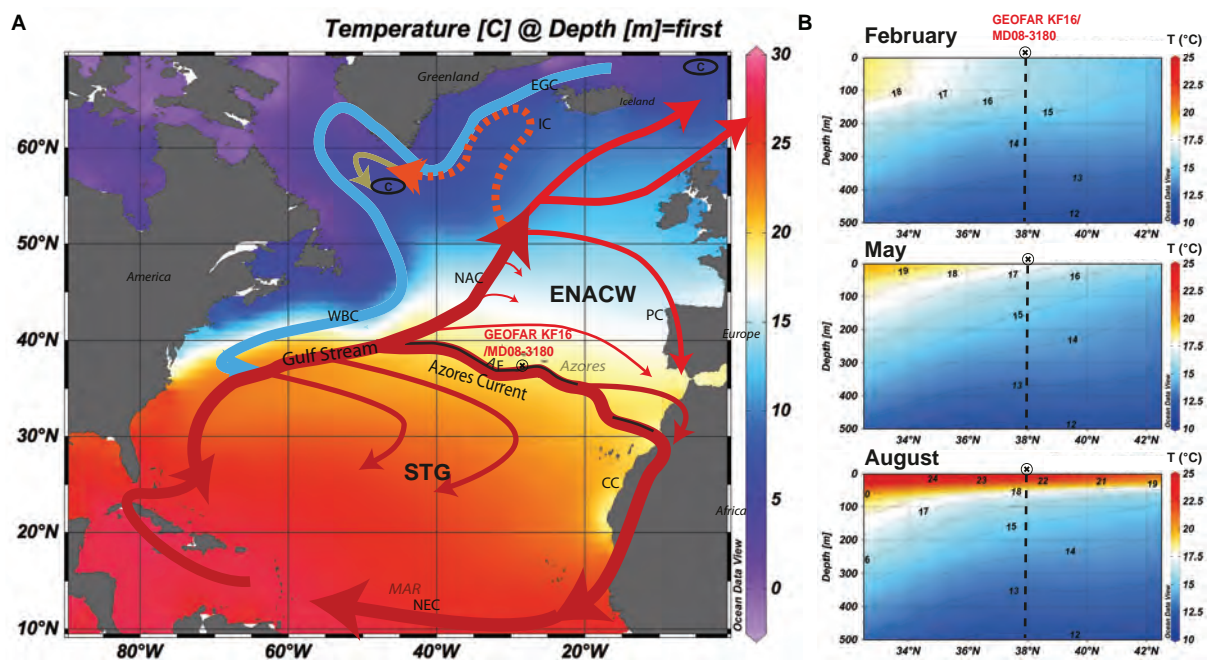


FIGURE 1

(A) Main surface (solid lines) and subsurface (hatched line) currents in the North Atlantic. Warm currents are displayed in red, cold currents in blue. Color shading refers to annual mean SST (Locarnini et al., 2013). AF Azores Front, CC Canary Current, EGC East Greenland Current, ENACW Eastern North Atlantic Central Water, IC Irminger Current, NAC North Atlantic Current, NEC North Equatorial Current, PC Portugal Current, STG Subtropical Gyre, WBC Western Boundary Current, C Deepwater convection sites. (B) Cross sections on the modern temperature distribution across the AF along 28°W displaying spring to summer conditions (Locarnini et al., 2013) plotted with ODV (Schlitzer, 2012).

bearing organisms might have a strong impact on the calculations and may overprint the actual calculated $\delta^{18}\text{O}_{\text{WATER}}$ ($\delta^{18}\text{O}_w$) values. This effect will be tested in the last paragraph of this paper.

2. Regional setting

The surface hydrography at the GEOFAR KF16/MD08-3180 coring site in the subtropical North Atlantic is governed by the Azores Front-Current System (Figure 1). The modern Azores Current (AC) branches off from the North Atlantic Current (NAC) between 30 and 40°N and meanders east, inducing mesoscale eddies (e.g., Käse and Siedler, 1982). Within this current system, the AF separates oligotrophic Subtropical Mode Water (SMW), and mesotrophic Eastern North Atlantic Central Water (ENACW) (Käse and Siedler, 1982; McCartney and Talley, 1982; Mason and Oliveira, 2006; Liu and Tanhua, 2019a,b). In newer publications, these water masses are also named tropical Eastern North Atlantic Central Water (ENACW_T) and subtropical North Atlantic Central Water (ENACW_P) (e.g., Mason and Oliveira, 2006; Liu and Tanhua, 2019a,b). Both SMW and ENACW are surface water masses (e.g., Liu and Tanhua, 2019b). The AF is defined by the position of the southward dipping 15°C-isotherm (Gould, 1985). Being a subsurface front overlain by the surface waters with relatively homogeneous SST (Alves et al., 2002), changes in SST across the AF cannot be used to trace the position of the AF. The divide between different surface dwelling planktic foraminifer assemblages is located between the SMW and ENACW to the north

of the AF (Ottens, 1991; Schiebel et al., 2002a; Rogerson et al., 2004) at about 34–38°N.

Under modern conditions, main phytoplankton production in the vicinity of the Azores occurs at increasing light-levels in early spring (March) and moves north to the transitional to subpolar NA (40 and 60°N) following photic conditions until June (Obata et al., 1996; Longhurst, 2007; Henson et al., 2009). Coccolithophore production in the mid-latitude North Atlantic may persist beyond maximum production of other phytoplankton groups, and enhanced coccolithophore diversity (i.e., number of species) may characterize the late spring to early summer succession in surface waters (e.g., Haidar and Thierstein, 2001; Schiebel et al., 2011; Hopkins et al., 2015; Poulton et al., 2017).

3. Materials and methods

A high-resolution deglacial record of the combined cores GEOFAR KF16 (37°59.59'N 31°7.698'W, 3050 m water depth) and MD08-3180 (37°59.99'N 31°8.07'W, 3064 m water depth) from a coring site situated to the southwest of the Azores at the northern boundary of the AF has been analyzed (Richter, 1998; Kissel et al., 2008; Schwab et al., 2012; Repschläger et al., 2015). A previously published age model is based on 15 Accelerator Mass Spectrometer (AMS) radiocarbon ages of monospecific planktic foraminifer samples, and refined by tuning the alkenone SST record to NGRIP ice core data (Schwab et al., 2012). The original age model has been modified by using the ^{14}C AMS plateau tuning technique (Sarnthein et al., 2015). Planktic foraminifer tests are

well preserved as shown by the occurrence of pteropods during the YD. Planktic foraminifer assemblage data were previously published by Repschläger et al. (2015) and Weinelt et al. (2015), and supplemented with new Holocene data (97 samples) in centennial resolution (see **Supplementary Table 1** for details). All planktic foraminifer counts were performed on a split of at least 300 individuals from the size fraction $> 150 \mu\text{m}$ following the taxonomy of Pflaumann et al. (1996), which is based on Bé and Tolderlund (1971).

Temperature reconstructions are compared for three different methods (1) planktic foraminifer transfer functions (SIMMAX) (Pflaumann et al., 1996), (2) alkenone SST reconstructions ($U^{K'}_{37}$ SST) (Schwab et al., 2013), and (3) Mg/Ca temperature reconstructions (Repschläger et al., 2015, 2017). For the Holocene, Mg/Ca and SIMMAX data were obtained from the same samples taken from core GEOFAR K16 and $U^{K'}_{37}$ records stem from core MD08-3180. For Bølling-Allerød (BA) and YD, all analyses were performed on samples from core MD08-3180. Both Mg/Ca and stable isotope analyses was performed on specimens of the size range $> 350 \mu\text{m}$.

SIMMAX (Pflaumann et al., 1996) were calculated using published planktic foraminifer assemblage data (Repschläger et al., 2015; Weinelt et al., 2015) and supplemented with unpublished Holocene planktic foraminifer assemblage data at decadal to centennial resolution. The used reference database SIMMAX28 consists of 947 core top samples that are linked to SST from the Levitus94 database (Levitus and Boyer, 1994). To calculate distant and non-distant weighted summer and winter SSTs the best ten analogs have been used. The minimum correlation coefficient of the default SIMMAX setting was reduced from 0.9 (90%) to 0.0 (0%) as the use of default settings resulted in non-analog situations for more than 30% of the samples. For the adjusted setting, the correlation coefficient is > 0.92 for all Holocene samples except samples around 8.2 ka BP, 9.3–9.6 and 10.4 ka BP with lower similarities. Samples older than 11.4 ka BP show correlations between 0.7 and 0.9. Within this study, not distant weighted results were used, as core top values better reproduce the modern situation. The difference to the distant weighted method does not exceed 0.5°C . The standard deviation of the SIMMAX SST reconstruction is $\pm 1^\circ\text{C}$.

The alkenone unsaturation index $U^{K'}_{37}$ (Prah and Wakeham, 1987) is calibrated against temperature using the calibration of Müller et al. (1998) and was published by Schwab et al. (2013). The Mg/Ca data from the size fraction $> 315 \mu\text{m}$ were previously published by Repschläger et al. (2015, 2017), the standard deviation of SST calculation for this core is $\pm 0.2^\circ\text{C}$ (Schwab et al., 2013) obtained from replicate measurements. The systematic error of the calibration used in this study is $\pm 1^\circ\text{C}$. Mg/Ca based temperature estimates from surface (*Globigerinoides ruber*, *Globigerina bulloides*) and subsurface dwelling (*Globorotalia truncatulinoides*) planktic foraminifers are calibrated with the equations given by Anand et al. (2003) (general equation for mixed planktic foraminifera species, eq. 5) and Cléroux et al. (2008) (eq. 1). These calibrations have been chosen from a variety of existing calibrations as their results give the best match for Late Holocene (LH) temperatures with the modern conditions at the AF (see **Supplementary Table 1**). Duplicate measurements of downcore samples result in a combined measurement and calibration with a standard deviation of $\pm 1^\circ\text{C}$ for *G. ruber* and *G. bulloides*,

and $\pm 2^\circ\text{C}$ for *G. truncatulinoides*. Mg/Ca measurements on *G. ruber* (Mg/Ca SST_{Gr}) have only been possible for the warm Allerød and Holocene. Low numbers of tests of *G. ruber* impede analyses of the cold intervals YD and H1. Mg/Ca was measured on *G. bulloides* over the late BA to late YD time interval. During the BA and Intra Allerød Cold Period (IACP) time intervals, several results had to be discarded due to mineral coatings indicated by anomalously high Fe content. Full analytical methods and errors of temperature reconstruction are presented in the original publications (Schwab et al., 2013; Repschläger et al., 2015, 2017; Weinelt et al., 2015). For transparency, all data compiled for this study can be found with original citations in the **Supplementary Tables 1–6**.

Abundances of planktic foraminifer species are used as indicators for additional evidence on hydrological changes at the Azores coring site: *G. ruber* [all white morphotypes combined for their common ecological significance (Yamasaki et al., 2022)] are tropical to subtropical surface-dwellers that typically thrive in waters warmer than 18°C (Bradshaw, 1957). Samples from core tops (Pflaumann et al., 1996), sediment traps, and plankton tows (Schiebel et al., 2002b) indicate a dominance of its abundance during late spring at 32°N , and a change to late summer conditions further to the North, and are associated with oligotrophic late summer conditions (Storz et al., 2009). Here, we assume *G. ruber* a is an indicator for the STG waters, with its variability in relative abundance reflecting changes in the AF position. Additionally, we propose that the Mg/Ca record of *G. ruber* reflects summer temperatures.

Deep-dwelling *G. truncatulinoides* are most abundant south of the AC system within the SMW realm. *G. truncatulinoides* is assumed to have an annual life cycle and to add a secondary calcite at thermocline depth before ascending for reproduction in the Azores region (Hemleben et al., 1989; Schiebel et al., 2002b). Surface and subsurface dwelling *Neogloboquadrina incompta* and *Globorotalia scitula* (Hemleben et al., 1989; Ottens, 1991; Schiebel et al., 2002a,b; Rebotim et al., 2017, 2019) typically occur north of the AF within the ENACW. Enhanced relative abundances of *G. scitula* are indicative of the northern water bodies (Schiebel et al., 2002a).

Surface to subsurface dwelling *Turborotalita quinqueloba* and *Neogloboquadrina pachyderma* (Rebotim et al., 2017, 2019) are most abundant in the Nordic Seas and at the Polar Front being valid indicators for subpolar to polar conditions (Bé and Tolderlund, 1971; Ottens and Nederbragt, 1992; Pflaumann et al., 1996; Simstich et al., 2003). *T. quinqueloba* is also associated to hydrologic fronts and occurs in high numbers at the warm side of the Arctic front (Johannessen et al., 1994; Husum and Hald, 2012). The cold-water species *N. pachyderma* (previously *N. pachyderma* left coiling) indicates the influence of subpolar waters at the coring site.

Globigerina bulloides and *Globigerinita glutinata* are most abundant in subpolar to transitional waters showing a bimodal abundance peaking in late spring and autumn (Schiebel and Hemleben, 2000; Schiebel et al., 2001; Jonkers and Kučera, 2015).

The planktic foraminifer $\delta^{18}\text{O}_c$ record (Repschläger et al., 2015, 2017; Balmer and Sarnthein, 2018) is corrected for the temperature effect, using SIMMAX, Mg/Ca and $U^{K'}_{37}$ temperature reconstructions and the Shackleton (1974) equation. This results in estimates for changes in past $\delta^{18}\text{O}_w$ composition. This signal has been further corrected for the ice-volume effect, using the relative

sea level composite curve of Austermann et al. (2013) to calculate $\delta^{18}\text{O}_{w\text{-ice}}$.

4. Results

The combined spliced sediment record spans the last 15.5 ka BP with a multidecadal to centennial resolution. It includes the last deglaciation with warm periods such as the BA and the Holocene, and cold periods such as H1 and YD events. The short-term cold Greenland Interstadial 1b at 13.1 ka BP, also known as Intra Allerød Cold Period (IACP) (Rasmussen et al., 2006, and references therein), and the 8.2-kyr-BP-Event interrupt the warm BA and Holocene, respectively. According to the SIMMAX and $U^{K'}_{37}$ derived SST estimates, the general temperature pattern follows the known deglacial succession with warm BA and Holocene temperatures, and cold H1 and YD temperatures (Bard, 2001a) in the North Atlantic. Yet, distinct differences are observed between records (Figure 2). In general, SIMMAX summer and winter temperatures show the same pattern of change with 5°C colder temperatures during winter in average. Smaller winter than summer cooling amplitudes during cold H1 and late YD/early Holocene are observed.

4.1. Heinrich event 1 (H1)

Coldest surface temperatures are observed during H1 in all surface temperature records. SIMMAX summer SST (SIMMAX SST_{su}) (Figure 2A) drop to 9°C, and thus indicate a summer cooling of 13°C with respect to modern SSTs. $U^{K'}_{37}$ SSTs indicate temperatures around 12.5°C (Figure 2B), with a cooling amplitude of 7.5°C that is less pronounced than in the SIMMAX record. Although calibrated to reflect annual mean SSTs, $U^{K'}_{37}$ temperatures during H1 are warmer than planktic foraminifer-based summer SSTs.

Globorotalia truncatulinoides based subsurface Mg/Ca temperatures (Mg/Ca T_{Gtrunc}) indicate temperatures of 14°C for H1, Figures 2C, 3E, H. Numbers of subtropical planktic foraminifers are low during H1, with relative abundances of *G. ruber* and *G. truncatulinoides* at <2% (Figures 3A, B), while the relative abundances of polar and subpolar species such as *N. pachyderma* (5%), *T. quinqueloba* (15–20%), and *N. incompta* (15–30%) (Figures 3C–G) are higher and increase toward the end of H1. Also, relative abundances of *G. scitula* are elevated (10–20%) in H1 in comparison to the preceding and following time-intervals (Figure 3C).

4.2. Bølling-Allerød (BA)

Bølling-Allerød interval is 5 to 9°C warmer than the H1 event with average $U^{K'}_{37}$ and SIMMAX SST_{su} of 19 to 20°C and match modern annual mean SST of 19°C (Figures 2A, B). SIMMAX SST_{wi} remain 5°C colder. Mg/Ca SST_{Gr} are only available for the late Allerød, indicating SST of 21.5°C close to LH SST. *G. bulloides* Mg/Ca SST (Mg/Ca SST_{Gb}) are similar to $U^{K'}_{37}$ derived SSTs, reaching modern winter SSTs of 17°C from Bølling to early Allerød (14.4–14.2 ka) (Figure 2C). Here, the IACP interval

in which Mg/Ca SST_{Gb} are overprinted by mineral coatings are excluded. Subsurface Mg/Ca temperatures of *G. truncatulinoides* (Mg/Ca T_{Gtrunc}) decrease from 16°C at the beginning of BA to 14°C at the onset of IACP (Figure 2C). Relative abundances of *G. ruber* were at intermediate values (10%) during BA (Figure 3A). The relative abundances of *N. incompta* (Figure 3F) show a pronounced peak (30–35%) at the onset of BA (12.6 to 12.4 ka BP). Relative abundances of polar/subpolar and temperate species *N. pachyderma* (0–2%) (Figure 3H), *T. quinqueloba* (5%) (Figure 3G), and *G. glutinata* (5–7%) (Figure 3F) are low. Relative abundances of *G. scitula* decrease from about 8 to 2% in early BA, at 14.5 ka BP, and remain low until IACP (Figure 3C).

The IACP, centered at 13.1 ka BP, interrupts warm BA with a pronounced cooling in the SIMMAX SST_{su} to 10°C, i.e., temperatures close to those estimated for the H1 event. The strong cooling in SIMMAX SST estimates coincides with a cooling signal of 1.5°C in the $U^{K'}_{37}$ record from 18.5 to 17°C, which is represented by a single data point only. Relative abundances of *T. quinqueloba* and *G. scitula* sharply increase to 30 and 14%, respectively (Figures 3C, G). After IACP, SSTs and abundance records return to average BA values, with the exception of relative abundances of *G. ruber* that remain low at <2% until the end of YD.

4.3. Younger Dryas (YD)

At the beginning of YD, 4°C cooling is observed in the $U^{K'}_{37}$ SST and Mg/Ca SST_{Gb} records (Figures 2B, C). After the initial cooling, both records range between 13 and 15°C. and Mg/Ca T_{Gtrunc} remain relatively warm with average values of about 14°C. Mg/Ca SST_{Gb} , $U^{K'}_{37}$ SST, and Mg/Ca T_{Gtrunc} provide similar temperatures that match modern winter temperatures and imply a collapse of the thermal surface water stratification. The exception in this pattern is the SST_{su} record that remains relatively warm (16°C) until 12.2 ka and cools down by 2 to 14°C thereafter (Figure 2A). Over the entire YD, SST_{wi} are 4°C colder than SST_{su} . During late YD, SIMMAX SST_{su} cools down by 4 to 14°C but still remains 2°C warmer than the $U^{K'}_{37}$ SST. The relative abundances of *G. ruber* a, *G. truncatulinoides*, *N. pachyderma*, and *G. scitula* are very low (<2%) during YD. The relative abundances of *N. incompta* show two peaks, one at the onset of the YD (37%) and one (40%) in late YD (Figure 3). Relative abundances of *T. quinqueloba* (Figure 3G) are slightly decreasing from 15 to 10%, and abundances of *G. bulloides* fluctuate by 15 around 30%. Abundances of *G. glutinata* vary between about 25 and 10% (Figure 3E).

4.4. Early Holocene

The general warming trend into the Early Holocene from average temperatures of 14°C during YD to 23°C at 9.5 ka BP in the SIMMAX SST is characterized by pronounced and rapid decadal fluctuations with magnitudes of about 4°C (Figure 2A). This short-term climate variability is not visible in the $U^{K'}_{37}$ SST record (Figure 2B). $U^{K'}_{37}$ SST rise in the beginning of the Early Holocene and reach modern annual mean SST of 19°C at 11.5 ka BP, and stay constant until the 8.2-ka-BP-Event. Mg/Ca SST_{Gr}

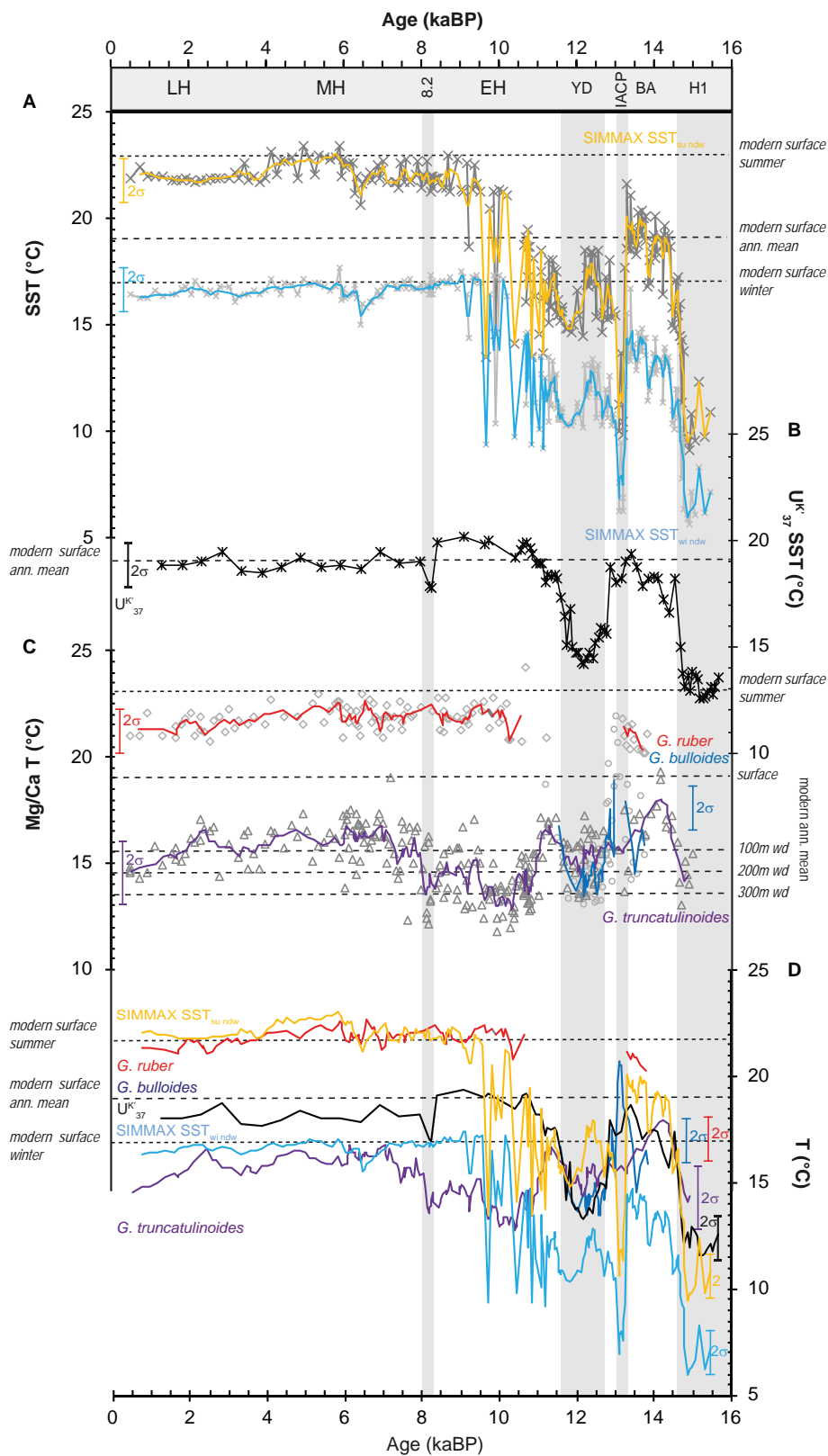


FIGURE 2

Comparison of SST reconstructions from different proxies spanning the Last Glacial (H1) to Late Holocene (LH) time period. **(A)** Non-distance weighted SIMMAX summer (yellow) and winter (light blue) SST records. **(B)** Alkenone U^{K}_{37} SST estimates (black) (Schwab et al., 2012). **(C)** Surface water Mg/Ca SST obtained from *G. ruber* (red line) and *G. bulloides* (dark blue line) (Repschläger et al., 2015, 2017) and subsurface temperatures reconstructed from *G. truncatulinoides* Mg/Ca (violet line) (Repschläger et al., 2015, 2017). **(D)** Comparison of temperature reconstructions. Modern surface temperatures are shown for reference in horizontal bars. Lines in Mg/Ca SST records display three-point running mean values. BA Bølling-Allerød, IACP Intra Allerød Cold Period, YD Younger Dryas, EH Early Holocene, 8.2 8.2-ka-BP-Event, MH Mid Holocene, wd water depth.

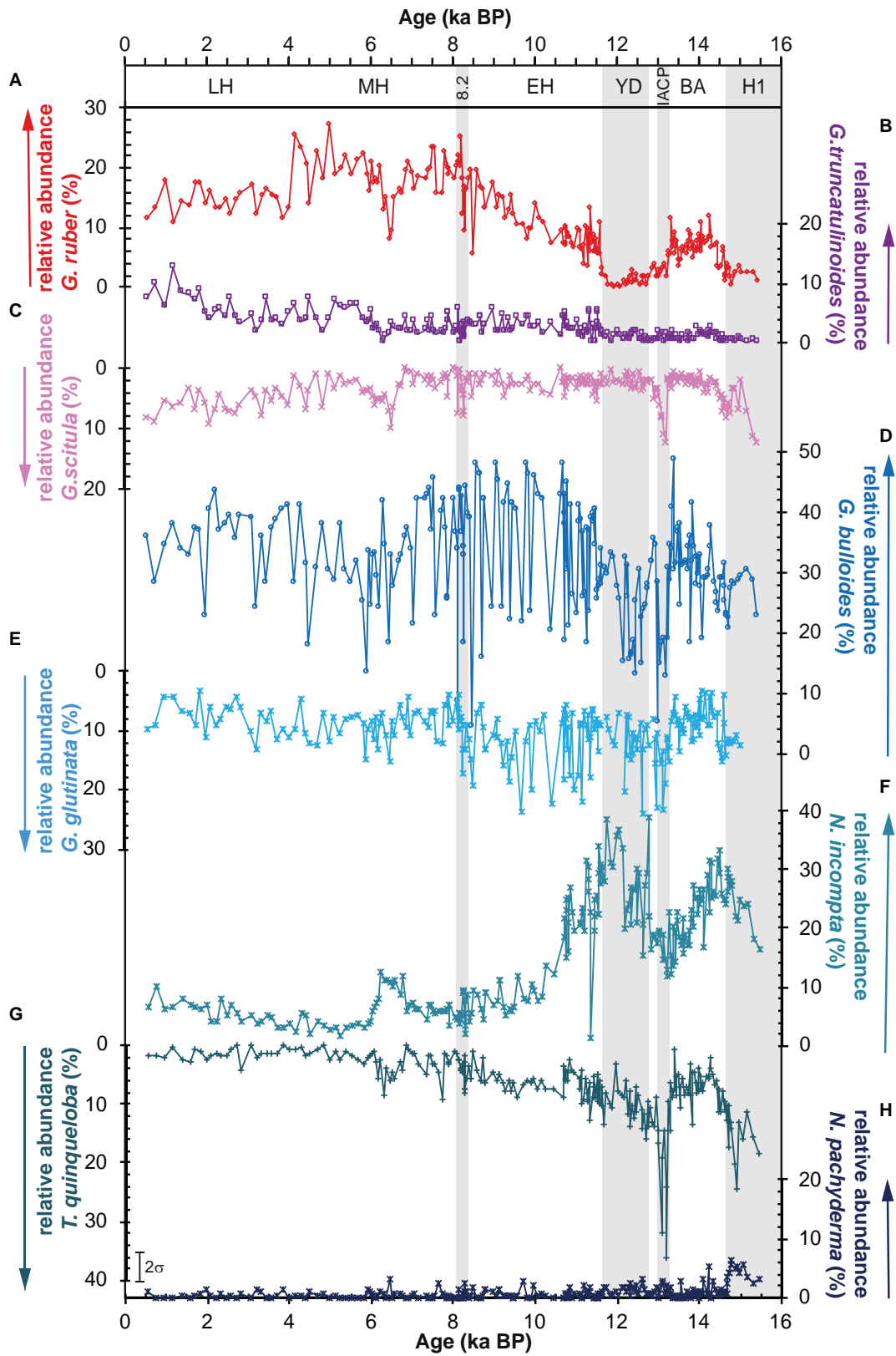


FIGURE 3
 Relative abundance records of subtropical species (A) *G. ruber* (red line), (B) *G. truncatulinoides* (violet), (C) *G. scitula* (pink), (D) *G. bulloides* (dark blue), (E) *G. glutinata* (light blue), (F) *N. incompta* (light green-blue), and sub/polar species (G) *T. quinqueloba* (dark green-blue), and (H) *N. pachyderma* (dark blue). Note that the y-axes of the temperate and subpolar species *G. scitula*, *T. quinqueloba*, *N. incompta*, and *N. pachyderma* are inversely plotted. For abbreviations on time axis see Figure 2.

indicates relatively stable SST of 23°C from 10.5 ka BP on. Short-term variability cannot be tested in the Mg/Ca SST_{Gr} and Mg/Ca SST_{Gb} records due to missing data for these events (Figures 2A, C). The Mg/Ca T_{Gtrunc} cool down to 12°C, reaching H1 values at the beginning of Early Holocene and show a long-term gradual increase into the 8.2-ka-BP-Event to 17°C. Relative abundances of *G. ruber* are at intermediate values (10%). Relative abundances of *G. truncatulinoides* fluctuate between 1 and 4% and are slightly increased compared to the YD to H1 interval before (Figure 3). Relative abundances of *N. pachyderma* (<2%) and *G. scitula* (1–6%) are low, *N. incompta* relative abundances steadily decrease from 40% at 11.6 ka and reach Holocene mean values of about 10% at 10 ka BP (Figures 3C, F, H). Relative abundances of *T. quinqueloba* (Figure 3G) slightly decrease from 10 to 5% and *G. bulloides* relative abundances vary by 10% around a mean value of 30% (Figure 3D). *G. glutinata* (Figure 3E) show similar variability of ± 9% around a mean of 15% with an inverse distribution to *G. bulloides*.

4.5. Mid- to Late Holocene

From the Mid to Late Holocene, SIMMAX SST_{su/wi} are close to modern summer (23°C) and winter surface temperatures (16°C). Over the past 9 ka, temperatures vary by 1°C being slightly warmer from 6.5 and 4 ka BP SST_{su/wi} and cooler from 9 to 6.5 ka BP and 4 to 0.5 ka BP. The temperature difference between summer and winter amounts to about 7°C during the entire Holocene (Figure 2A). The U^{K'}₃₇ SST record resembles the annual mean SSTs over the Holocene (19°C) with an SST maximum between 11 and 8 ka BP, following maximum northern hemisphere summer insolation (Figures 2B, 4). Mg/Ca SST_{Gr} indicate SSTs of 21–22°C, slightly below modern summer SSTs (Figure 2C). Mg/Ca T_{Gtrunc} fluctuates around an average of 14°C coinciding with modern subsurface temperatures at 200 m water depth.

G. ruber reach maximum relative abundances of about 25% between 8 and 4 ka BP (Figure 3A). After 4 ka BP, the abundances stabilize on LH values between 14 and 18%. The relative abundances of *G. truncatulinoides*, *G. scitula*, and *N. incompta* increase from 7 ka (2%) until the end of the Holocene (10%) (Figures 3B, C, F). Abundances of *G. bulloides* strongly fluctuate around an average of 32% (Figure 3D), while relative abundances of the polar and subpolar species *N. pachyderma* (<2%) and *T. quinqueloba* (<5%) are low during the entire Mid- to Late Holocene (Figures 3G, H). Abundances of *G. glutinata* fluctuate around 7% and seem to follow a systematics different from *G. bulloides* (Figures 3D, E).

5. Discussion

5.1. Reliability of records

Mg/Ca temperature reconstructions from planktic foraminifer shells are affected by seasonal changes in productivity, species specific water depth habitats, and the analyzed test size fractions (Skinner and Elderfield, 2005; Chapman, 2010; Schneider et al., 2010; Lombard et al., 2011; Friedrich et al., 2012; Lohmann et al.,

2012; Rebotim et al., 2017), as well as changes in the chemistry of ambient seawater including salinity (Kisakürek et al., 2008; Mathien-Blard and Bassinot, 2009; Sabbatini et al., 2011), and carbonate ion concentration (Arbuszewski et al., 2010; Evans et al., 2016; Gray et al., 2018). Furthermore, trace element coatings of planktic foraminifer shells can strongly affect the Mg/Ca signature (Barker et al., 2003; Bian and Martin, 2010). Reduced reliability of the Mg/Ca temperature calibration at the cold end of the calibration dataset might lead to an overestimation of the SSTs lower than about 5°C (Meland et al., 2005; Kozdon et al., 2009). These factors will be addressed in the following.

A variety of calibration functions to transfer Mg/Ca from foraminifer shell calcite into temperature are available. These functions are based on cultured individuals (Nürnberg et al., 1996; Kisakürek et al., 2008), sediment trap data (e.g., Anand et al., 2003; McConnell and Thunell, 2005), and core top data (e.g., Elderfield and Ganssen, 2000; Lea et al., 2000; Dekens et al., 2002; Cléroux et al., 2007, 2008; Regenberg et al., 2007) including multispecies (Elderfield and Ganssen, 2000; Anand et al., 2003) and monospecific approaches (Elderfield and Ganssen, 2000; Lea et al., 2000; Dekens et al., 2002; Cléroux et al., 2007, 2008). The use of different calibration functions results in offsets between the calculated Mg/Ca temperatures (Supplementary Figure 1). Thereby, differences in calibration functions affect the slope and intercept of the calibrations, leading to differences in the absolute temperatures of 1–4°C for *G. ruber*, 0.1–1.8°C for *G. bulloides*, and 2.8–7.9°C for *G. truncatulinoides* (Supplementary Figure 1). Within this range of temperature estimates, some result in unreasonably high or low temperature reconstructions for the core top samples at our coring site, and can thus be excluded. The differences of absolute temperature estimates of residual calibrations are within the range of the calibration uncertainty. From all calibrations, downcore amplitudes of change in Mg/Ca temperatures from *G. ruber* and *G. bulloides* differ by less than 1°C, and by 0.5–1.4°C in *G. truncatulinoides*. These differences in amplitude are well within the standard deviation of the calibrations.

The differences in absolute temperatures have been explained by various effects. Differences in ontogenetic stage are shown to have a major effect on the Mg/Ca and δ¹⁸O values in planktic foraminifers (Friedrich et al., 2012). This is especially important for shell sizes below 250 μm. The shell sizes used in this study are >315 μm and calibration functions obtained from similar shell sizes were used. Thus, shell size dependant offsets can be regarded as minor and will not be addressed in the following discussion.

Differences between core top, culture, and sediment trap calibrations are explained by early diagenesis in the sediments (Regenberg et al., 2007; Hertzberg and Schmidt, 2013). By addition of gametogenic calcite on the shells that only becomes evident in foraminifers that underwent the full life cycle. These differences may not occur in plankton tow samples (Jentzen et al., 2018). In addition, many core top calibrations infer the dwelling depth of foraminifers by comparing foraminifera δ¹⁸O values with calculated δ¹⁸O calcite (δ¹⁸O_c) data (e.g., Regenberg et al., 2009). These values are calculated in two steps. Due to a lack of δ¹⁸O measurements in the water column (δ¹⁸O_w), δ¹⁸O_w is calculated from salinity measurements using local salinity- δ¹⁸O_w conversions. In a second step, δ¹⁸O_c values are calculated using species specific equations that convert δ¹⁸O_w under consideration of water temperature into theoretical δ¹⁸O_c for all water depths.

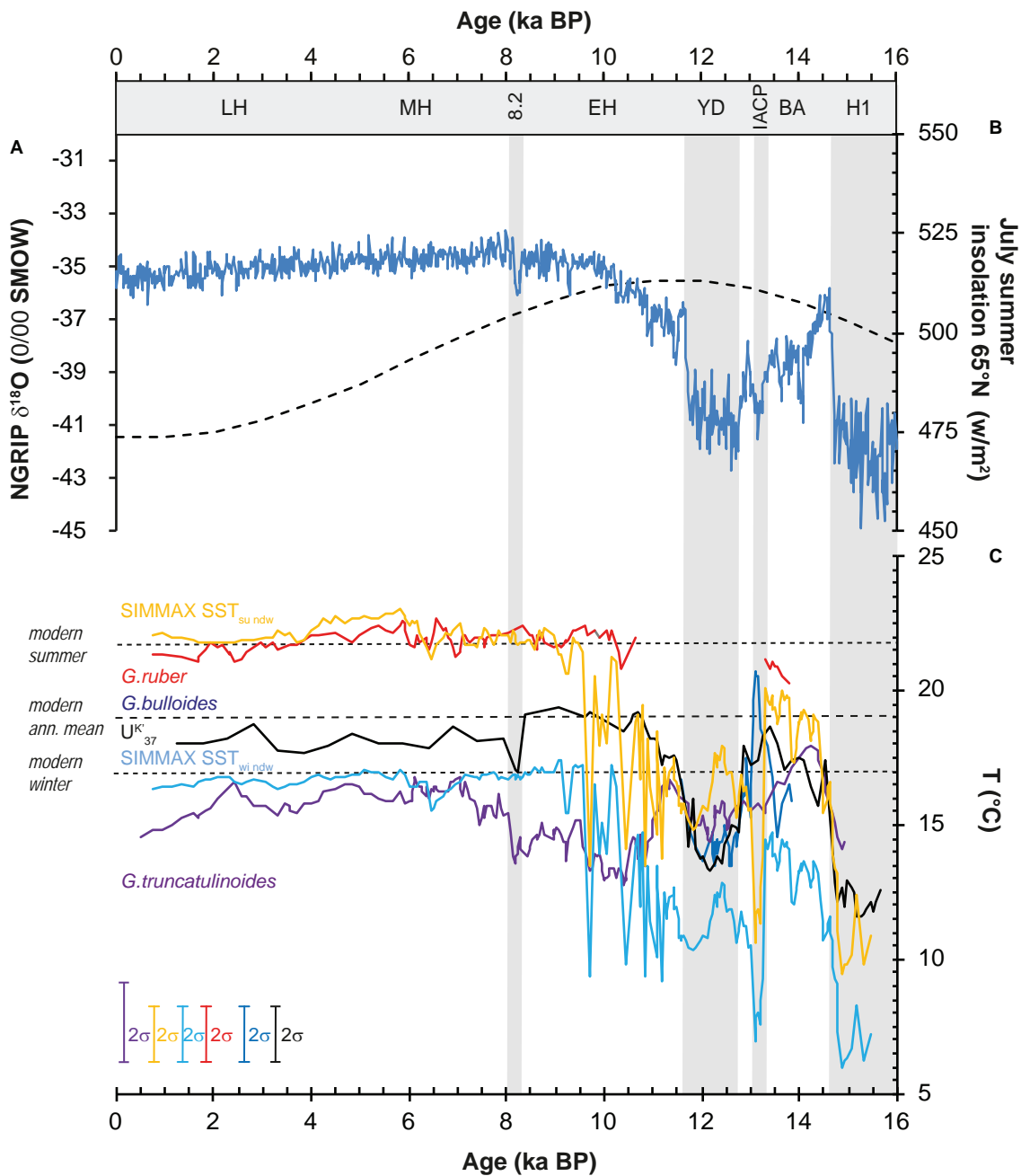


FIGURE 4

Comparison of (A) ice core record NGRIP $\delta^{18}O$ (Andersen et al., 2006), and (B) northern hemisphere summer insolation changes (Berger and Loutre, 1991), with (C) deglacial SST reconstructions based on non-distance weighted SIMMAX summer (yellow) and winter (light blue) SST, Alkenone $U^{K'}_{37}$ SST (black) (Schwab et al., 2012), and planktic foraminifer Mg/Ca SST (Repschläger et al., 2015, 2017). Lines in Mg/Ca SST records display three-point running mean values. For abbreviations on time axis see Figure 2, a single data point excursion of 1°C during the IACP in the $U^{K'}_{37}$ SST record is not reliable.

The comparison of $\delta^{18}O_c$ with the actual $\delta^{18}O$ measurements in the foraminifers is used to infer the dwelling depth of the foraminifer. This practise has several weaknesses: The conversion from salinity into theoretical $\delta^{18}O_w$ data neglects seasonal variability, and water mass differences in the $\delta^{18}O_w$ to salinity relationships (McConnell et al., 2009). For conversion of $\delta^{18}O_w$ into $\delta^{18}O_c$, a wide range of different formula are available, resulting, for example, in calculated calcification depths of the upper 80 m for *G. ruber* and 200 m for *G. truncatulinoides* (Regenberg et al., 2009). Furthermore, the use of

annual data for the calibration neglects differences in the seasonal abundance of foraminifers, and associated changes in ambient water temperature and salinity.

Differences in calculated calcification depths transfer, for example, to 4°C temperature differences in the subtropical North Atlantic that are reflected in the absolute SST difference calculated by the various Mg/Ca calibrations. The effect of (neglected) seasonality in calibration functions may account for temperature differences of up to 4°C for *G. ruber* and 2°C for *G. truncatulinoides*

(Regenberg et al., 2009). Furthermore, most calibrations are focused on ocean basins rather than using global datasets to account for differences in ocean chemistry (e.g., Lea et al., 2000).

Given the multiple effects that lead to the observed differences between sediment traps, living foraminifers, and core top samples, as well as differences between ocean basins, in the following we only consider calibrations from the Atlantic Ocean basin. In agreement with other studies, we chose the calibration function of Anand et al. (2003) that represents the closest match between the modern observations and core top data considering that *G. ruber* reflects late summer conditions in the upper 30–50 m (Schiebel et al., 2002b; Storz et al., 2009; Rebotim et al., 2017). The evaluation of Mg/Ca calibrations on *G. bulloides* are impeded by the lack of core top data. In this case, we chose the calibration from the same North Atlantic core top dataset as for *G. ruber* (Anand et al., 2003). Based on the plankton tow and sediment trap data we assume that *G. truncatulinoides* match the calibration of Cléroux et al. (2007).

In addition to early diagenesis, an underestimated influence of salinity and carbonate chemistry (pH and CO_3^{2-} concentration) on the Mg/Ca incorporation (Gray et al., 2018; Gray and Evans, 2019) might have an effect on the SST reconstructions. These effects have to be addressed for the downcore samples, though core top and Late Holocene SST reconstructions match well with modern conditions. However, SEM images of the coccolithophores (Schwab, 2013) show good carbonate preservation at our coring site MD08-3180, and argue against effects of early diagenesis (Schwab, 2013). Following Hertzberg and Schmidt (2013), we assume that carbonate dissolution had no major effect on the preservation of foraminifer shells at our coring site as well.

At the coring site southwest of the Azores, glacial-to-interglacial variability in salinity and pH may account for decreased surface water temperatures of 1–1.5°C for *G. ruber* and *G. bulloides*, in comparison to model data shown by Gray and Evans (2019). This discrepancy is slightly exceeding the already considered combined error of measurement and calibration. Corrections for salinity and pH are hampered by the lack of independent salinity estimates, and pH reconstructions bear the risk of additional uncertainty arising from uncertainties in the pH reconstructions of ± 0.1 pH units (Raitzsch et al., 2018). The latter is in the same range as the uncertainty when using uncorrected data. Therefore, we did not apply any salinity and pH correction to our data. However, underestimation of the effects of pH and salinity could result in an underestimation Mg/Ca SST of 1°C, and would lead to an overestimation of the glacial-to-interglacial SST amplitude in all Mg/Ca SST estimates, and underestimate the difference to the alkenone SST record. To conclude, we assume that interspecies Mg/Ca SST temperature amplitudes are robust, whereas the error in absolute SST estimates might be higher than the $\pm 1^\circ\text{C}$ standard deviation of Mg/Ca measurements in *G. ruber* and *G. bulloides*, and differences to the alkenone SST record might be underestimated.

To transfer alkenone records into SST, two different indices can be used: The U^{K}_{37} index including the 37:2, 37:3, 37:4 alkenones, while the $U^{K'}_{37}$ index includes 37:2 and 37:3 only. Ocean-basin specific calibrations are available. The effect of 37:4 on our SST calculations has already been tested by Schwab et al. (2012). The U^{K}_{37} Index based SST calculations, as well as the North Atlantic calibration set (Muñller et al., 1998) in H1 provide 1°C colder SSTs than $U^{K'}_{37}$ based SST reconstructions. These calibration

differences are within the standard deviation of $\pm 1^\circ\text{C}$ and can be regarded as a minor effect.

Although calibrated to defined water depths (here 10 m) in the surface mixed layer, SST reconstructions with the modern analog technique using SIMMAX (Pflaumann et al., 1996) might be affected by a strong imprint of subsurface (below thermocline) water mass conditions (Adloff et al., 2011; Telford et al., 2013). This is caused by the addition of species from different water depths in fossil planktic foraminifer assemblages, thus integrating the thermal structure of the whole upper water column. As long as the thermal structure of the upper ocean is stable, planktic foraminifer assemblages reflect SST. A change in the structure of the water column may have a stronger effect on the subsurface dwelling species than surface dwellers, and lead to a bias in the resulting temperature signals toward a subsurface water signal. This bias is especially important in regions with pronounced oceanographic changes between glacial and interglacial times that lack analog situations in the calibration datasets (Storz et al., 2009; Adloff et al., 2011; Telford et al., 2013). One of these regions is the northern boundary of the North Atlantic Subtropical Gyre (STG) where strong fluctuations of the AF are observed (Repschläger et al., 2015) that cause non-analog situations.

Biases in the transfer functions by non-analog conditions to the calibration dataset are highly possible given the non-analog character of our samples (see section “3. Materials and methods”). Thus, in the following, we rather address the feasibility of calculated SST estimates than discuss absolute SSTs. Estimates of winter temperatures and seasonal differences are most probably not independent due to a strong dependence on the summer dataset of calibration (Kucera et al., 2005). Thus, we assume that winter temperatures are less reliable. The differences in seasonal temperature amplitudes obtained from SIMMAX as well as SIMMAX winter SST estimates are not discussed in the following, and are presented for completeness of the classical SIMMAX approach only (Figures 2, 6).

5.2. Differences between Mg/Ca SST, SIMMAX SST, and $U^{K'}_{37}$ temperatures during the warm Late Holocene and BA time-intervals

Reconstructed average Mg/Ca SST_{Gr} of 20.8°C during BA, and 21.8°C during Late Holocene differ in 1°C, and can be assumed similar, when considering an error of $\pm 1^\circ\text{C}$ in SST estimates (Supplementary Figure 3).

Average $U^{K'}_{37}$ SST of 18.5°C in BA are similar to Mg/Ca SST_{Gb}, yet 2.3°C cooler than Mg/Ca SST_{Gr}. Although both Mg/Ca SST_{Gr} and $U^{K'}_{37}$ SST warm to 21.8/21.9 and to 19.2/18.9°C, respectively, during early/late Holocene, the difference between average Mg/Ca SST_{Gr} and $U^{K'}_{37}$ SST reconstructions increases to 2.7°C in early Holocene and to about 2.9°C during the Late Holocene. Average Mg/Ca SST_{Gr} are 3.3°C warmer than SIMMAX SST_{su} during BA, and are similar during Late Holocene. To explain these differences, we need to understand the differences in ecology of the proxy bearing organisms.

Observational data show maximum production of *G. ruber* in the modern subtropical to temperate North Atlantic following

overall enhanced primary productivity in late spring, and maximum relative abundances in late summer (Hemleben et al., 1989; Wolfeich, 1994; Schiebel et al., 2002b; Storz et al., 2009; Salmon et al., 2015; Schiebel and Hemleben, 2017). This finding is corroborated by results from ecological planktic foraminifer models for the modern situation (Kretschmer et al., 2018), and indicate similar phenology of *G. ruber* during glacial and interglacial times (Fraile et al., 2009; Lombard et al., 2011). Bearing photo-symbiosis, the dwelling depth of *G. ruber* is limited to the upper photic zone (e.g., Hemleben et al., 1989; Rebotim et al., 2017) with an average dwelling depth of 50 m in the Azores region (Schiebel et al., 2002a,b). Mg/Ca SST_{Gr} reconstructions of 21.5°C for late Holocene match well with late July SST at the coring site. Relative stable Late Holocene and BA Mg/Ca SST_{Gr} of 21.5 to 21.0°C indicate only small changes in water temperatures recorded by *G. ruber* for both time-intervals. This can either be associated to similar SST conditions, or to a change in the abundance maximum of *G. ruber* toward late August in BA. To test both possibilities, we compare the Mg/Ca SST_{Gr} record to the other SST calculations (Figures 4, 6).

The 2.8°C warmer Mg/Ca SST_{Gr} than U^{K'}₃₇ SSTs during the BA and Early Holocene are readily explained by the differential ecologies of the foraminifer species *G. ruber* and alkenone producing coccolithophores, respectively (Figure 4 and Supplementary Figure 3). Main coccolithophore production in the subtropical to subpolar North Atlantic occurs slightly after the observed annual chlorophyll maximum at the end of March until early June (Henson et al., 2009; Narciso et al., 2016). Coccolithophores need light to perform photosynthesis and thus are bound to the euphotic zone. U^{K'}₃₇ SST reconstructions match well with modern SST during end of May at 0–50 m water depth, Figure 1B, i.e., the average depth habitat of the regionally most abundant coccolithophore species *Emiliania huxleyi* (Haidar and Thierstein, 2001; Schiebel et al., 2011). Thus, we assume that U^{K'}₃₇ SST represent late May surface temperatures in the Azores region. While U^{K'}₃₇ is calibrated to match mean annual SST, it displays the spring SST in the Azores region. The difference between late May and July/August SST at the Azores coring site explains the general difference in Mg/Ca SST_{Gr} and U^{K'}₃₇ SST of 2.8°C. The decrease in the SST difference during BA to 2.3°C most probably is related to a slight shift of the phenology of the coccolithophore bloom toward later in the year or to slightly warmer spring temperatures during BA. A phenology change is proposed to occur during positive phases of NAO (Henson et al., 2009) and may argue for a NAO⁺ like pattern during BA that needs to be tested in future projects.

Mg/Ca SST_{Gb} match well with U^{K'}₃₇ SSTs during BA and YD. Observations and modeling studies (Schiebel et al., 1997, 2002a; Rebotim et al., 2017; Kretschmer et al., 2018) suggest that *G. bulloides* mainly dwells in the upper 60 to 100 m in the temperate North Atlantic. As *G. bulloides* does not form major secondary calcite, it can be assumed that calcification depth does not differ from this water depth interval (Schiebel et al., 1997). Average Mg/Ca SST_{Gb} of 15.5°C in BA match well with modern SST observed in the upper 60 to 100 m water depth at the end of April. The depth habitat of *G. bulloides* is mainly controlled by food availability that coincides with the distribution of phytoplankton (Schiebel et al., 2001; Wilke et al., 2009). *G. bulloides* is feeding on diatoms from the early phytoplankton

spring bloom that occurs slightly before major mass production of coccolithophores at the end of spring (Schiebel et al., 1995; Poulton et al., 2017). Thus, we assume that Mg/Ca SST_{Gb} and U^{K'}₃₇ SSTs reflect the same season, i.e., spring, with a short time lag between the maximum abundances of both species *G. bulloides* and *E. huxleyi*.

Comparison of Mg/Ca SST_{Gb} and U^{K'}₃₇ SSTs with the Mg/Ca T_{Gtrunc} shows a unique temperature development between surface and subsurface waters. Mg/Ca T_{Gtrunc} during BA is warmer than the Mg/Ca SST_{Gb} and reaches similar values as under modern conditions at 100 m water depth (Repschläger et al., 2015). In combination with stable isotope data this phenomenon has been ascribed to subsurface warming, which may also have had an influence on temperatures of the overlying water column and may explain the reduced difference between Mg/Ca SST_{Gr} and U^{K'}₃₇ SSTs during BA in comparison to the Holocene.

Despite small temperature differences between Late Holocene and BA reconstructed from Mg/Ca (1°C) and U^{K'}₃₇ (0.4°C), the SIMMAX SST record indicates a 2.5°C difference between both time intervals (Supplementary Figure 3). During Mid and Late Holocene, SIMMAX SST_{su} (Supplementary Figure 3) match well with Mg/Ca SST_{Gr}. In contrast SIMMAX SST_{su} are 2°C cooler than Mg/Ca SST_{Gr} during BA and are close to U^{K'}₃₇ SST reconstructions from H1, to Early Holocene, instead.

This indicates that SIMMAX SST reconstructions react in a different way to AF position changes than the other proxies. This could be caused either by an underestimation of Mg/Ca SST_{Gr}, Mg/Ca SST_{Gb} and U^{K'}₃₇ SST amplitudes or by an overestimation of the cooling amplitude by SIMMAX SST.

An overestimation of the alkenone SST has been proposed in previous studies: A similar change in the alkenone signal with respect to SIMMAX SST has been observed in records from the Mediterranean Sea, the eastern African margin, and in the subpolar North Atlantic (Chapman et al., 1996; Sikes and Keigwin, 1996; Sicre et al., 2013), and has been explained with a change in growth period of the alkenone producing coccolithophores from late spring to summer. A change in the coccolithophore growth period could be explained by changes in the water mass properties (e.g., nutrient concentration, temperature, stratification) associated with (1) overall climate forcing such as a change in insolation (Leduc et al., 2010), or (2) a change in the position of hydrographic fronts (i.e., the AF).

(1) Previous work suggests a change in seasonality of the coccolithophores from summer to spring conditions during periods of insolation maxima (Leduc et al., 2010). The time period between H1 and Early Holocene coincides with the period of maximum summer insolation (Berger and Loutre, 1991; Figure 4). To explain the record at the AF, a change of the coccolithophore bloom from spring to summer during the insolation maximum and back to spring conditions after the summer insolation maximum would contradict this concept and seems unlikely. Furthermore, the Holocene cooling trend that is observed in subpolar North Atlantic U^{K'}₃₇ SST records and has been associated with insolation changes (Leduc et al., 2010) is missing in the Azores record.

(2) Southward displacements of the AF position are indicated by both decreased *G. ruber* abundances (Figure 3A), and elevated primary productivity (PP) during H1 and YD (Schwab et al., 2012). The pattern of change matches the succession of the deglacial warm and cold events and points to a southward change of the AF during

deglacial cold events. The divergence of the SIMMAX SST_{su} and U^{K'}₃₇ SST record appears between the Early and Mid-Holocene. This timing does not match with the strong deglacial oscillations in the AF position.

In addition to the major displacements of the AF during cold events, an increased influence of nutrient rich ENACW on the coring site could have had an impact on the phytoplankton bloom and facilitate a late plankton bloom and thus change in the U^{K'}₃₇ SST seasonality from summer to spring. An increased abundance of *N. incompta* (10–30%) (Figure 3E) is observed at the coring site from H1 to 10.5 ka BP. *N. incompta* typically occurs in high numbers in the modern ENACW (Schiebel et al., 2002a,b). Therefore, it can be assumed that more nutrient rich transitional ENACW prevailed at the coring site during this period coincident with the time period of similar SIMMAX SST_{su} and U^{K'}₃₇ SSTs (Figure 4). This may be an indicator of a change in the timing of phytoplankton production. Under modern conditions, the delay in coccolithophore production of positive vs. negative NAO phases in the subtropical North Atlantic is about 3 weeks (Henson et al., 2009) and relates to 0.5°C warmer temperatures at 50 m water depth. When added to the observed U^{K'}₃₇ SST amplitude of 0.4°C, the overall amplitude of 0.9°C U^{K'}₃₇ SST could be assumed and would be in the same range as the amplitude observed in Mg/Ca_{Gr}. Thus, a dampening of the overall alkenone SST amplitudes by a change in phenology is not unlikely for the time period between H1 and 10.5 ka BP.

Yet, the calculated amplitudes would still be much smaller than the SST difference of 2.2°C as reconstructed from SIMMAX SST_{su} between Holocene and BA. Therefore, the observed match between U^{K'}₃₇ SSTs and SIMMAX SST_{su} between H1 and Early Holocene, and its shift toward a match between Mg/Ca SST_{Gr} and SIMMAX SST_{su} in the Early Holocene cannot be solely explained by changes of the growth period of the coccolithophores, *G. ruber*, and *G. bulloides*. If this would be true, the SIMMAX SST_{su} record would produce too low SSTs. This could be caused by missing analog situations within the calibration dataset (Storz et al., 2009; Telford et al., 2013) possibly because mixed planktic foraminifer assemblages that represent hydrographic fronts are underrepresented in the SIMMAX calibration dataset (Storz et al., 2009). This becomes evident when regarding the similarity index below 0.9% calculated by SIMMAX for the interval between H1 and Early Holocene. To test the influence of the calibration dataset, SIMMAX calculations additionally were carried out using the updated and extended calibration dataset for the North Atlantic of Siccha and Kucera (2017). The new results are similar to the previous results, indicating that the underrepresentation of hydrographic front environments is not the controlling factor for the dissimilarities. Non-analog situations may occur over the entire down core record from the Azores Front-Current System, due to the inclusion of subpolar elements, and (cold) subsurface elements. Relatively cold SIMMAX SST_{su} are recorded during periods with elevated relative abundances of *N. incompta* (10–30%) (Figure 5) and decreased relative abundance of *G. ruber*. *Neogloboquadrina incompta* typically occurs in high numbers in the ENACW, and it can be assumed that ENACW prevailed at the coring site during BA. This water mass signal seems to overprint the SST signal in the SIMMAX calculations and leads to an underestimation of the SST at the coring site.

The strong effect of water mass properties other than temperature on the SIMMAX record is tested in the following by comparing the different SST reconstructions during cold periods with even stronger changes in the planktic foraminifer assemblage composition.

5.3. Differences in reconstructed temperatures during cold events

Centennial to decadal-scale cold events such as H1 and IACP are associated with extreme cooling in the SIMMAX SST record (Figure 2A). Especially during the short-term IACP cold event, only the SIMMAX SST_{su} record shows significant cooling with temperatures 5–6°C colder than U^{K'}₃₇ SST reconstructions (Figures 2, 4). Unfortunately, low abundances in *G. ruber* and an overprint by Fe-rich crusts on *G. bulloides* shells impede the comparison with Mg/Ca SST data during IACP and H1. The mismatch between SIMMAX SST_{su} and U^{K'}₃₇ SST might either be caused by a bias of U^{K'}₃₇ toward warm temperatures, admixture of transported alkenones from warmer regions (Mollenhauer et al., 2005), or non-analog conditions that result in anomalously low SIMMAX SST for the cold IACP event.

An underestimation of the cooling in the U^{K'}₃₇ SST in comparison to SIMMAX SST_{su} caused by an extreme increase in the abundance of the 37:4 component during cold events that is not considered in the U^{K'}₃₇ calculations has been excluded by Schwab et al. (2012) as already discussed above (see section “5.1. Reliability of records”). The weaker cooling suggested by the U^{K'}₃₇ SST could also be caused by lower sampling resolution compared to that of the foraminifer counts not resolving decadal-scale variability. We tested this hypothesis using the same sampling resolution for SIMMAX SST and the U^{K'}₃₇ SST record (Supplementary Figure 2). At lower resolution, the IACP cooling in the SIMMAX SST remains evident in two data points, indicating that the missing cooling signal is not caused by resolution.

It has been widely discussed that the alkenone temperature signal is smoothing-out short-term SST variability (Bard, 2001b; Ohkouchi et al., 2002; Mollenhauer et al., 2005; Leduc et al., 2010; Laepple and Huybers, 2014). This smoothing might either be related to the large amount of coccolithophore specimens contributing to the alkenones preserved in the sediments (Leduc et al., 2010; Laepple and Huybers, 2014), while about 400 foraminifers per sample are enumerated for the SIMMAX estimation. The smoothing may also be related to differential transport of coccolithophores and foraminifers with ocean currents (Ohkouchi et al., 2002; Mollenhauer et al., 2005), differential sedimentation, and bioturbation (Bard, 2001b). Parallel changes in coccolithophore (Schwab et al., 2012) and planktic foraminifer assemblages show pronounced abundance peaks of transitional to subpolar species during IACP, and indicate that transport-related biases between coccolithophores and planktic foraminifer are unlikely. The coinciding records as well exclude bioturbation as the cause of differential U^{K'}₃₇ SST and SIMMAX records. A third explanation arises from the modern structure of the AF. Under modern conditions, only a weak temperature gradient is observed in the surface waters at the AF (Alves et al., 2002). Thus, a strong temperature imprint just might be missing in the Alkenone record.

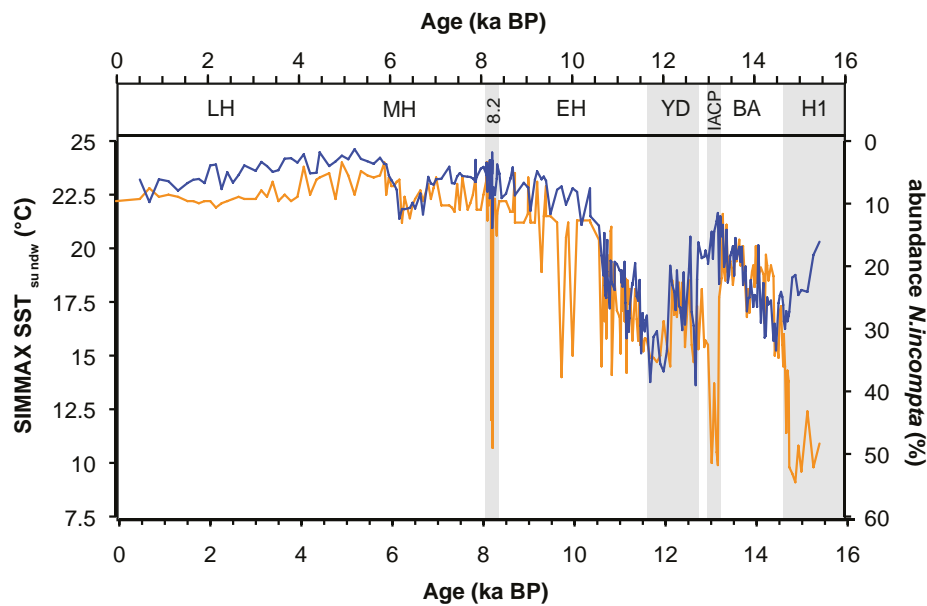


FIGURE 5

The comparison between SIMMAX SST_{su} (orange) and the relative abundance of *N. incompta* (blue) indicates a strong effect of *N. incompta* on the SIMMAX SST reconstructions.

In contrast, the SIMMAX_{su} SST react very sensitive to changes in the foraminifer assemblage composition that are associated with the southward displacement of the AF.

In the following, we interpret the missing cooling signal of the short-term events in the alkenone record as smoothing and lack of an SST gradient across the front. Still, the probability of an underestimation of SIMMAX SSTs during the cold H1 and IACP event needs to be explained.

The possibility of receiving too cold temperatures with the SIMMAX method due to an underrepresentation of mixed planktic foraminifer assemblages from hydrographic fronts in SIMMAX calibration datasets is likely, as discussed above. These non-analog situations of the down core data from the Azores-Front Current-System are evident from low similarities of 0.7–0.85 of the SIMMAX SST calculations (Supplementary Table 2) over the IACP interval, and need to be regarded with care (Pflaumann et al., 1996). More detailed analyses of the faunal assemblage during this IACP interval may help to understand the cause for the dissimilarities.

The cooling of the SIMMAX SST record (Figure 2A) of the IACP event is paralleled by high abundances of *T. quinqueloba* (Figure 3F) and the temperate subsurface species *G. scitula* (Figure 2D; Schiebel et al., 2002a). It is likely that the abundances of these species cause cold SIMMAX SST excursions during the IACP. High relative abundances of *T. quinqueloba* in the modern ocean with up to 20% are found in the NA (Schiebel and Hemleben, 2000). Relative *T. quinqueloba* abundances of 30–35% are observed in bottom sediments and sediment trap samples in the Nordic Seas (65°N) and southeast of Greenland (52°N) (Pflaumann et al., 1996; Jonkers et al., 2013). Maximum relative *G. scitula* frequencies of 7% prevail in sediment samples between 40 and 43°N (Pflaumann et al., 1996). In the subtropical North Atlantic, typical relative abundances of *T. quinqueloba* are in the range of 10–15% (Schiebel, 2002). High relative abundances of *T. quinqueloba* either reflect

colder conditions or a change in the sedimentation of tests of *T. quinqueloba* during IACP event. A change in sedimentation of tests of *T. quinqueloba* could have been caused by changes in the water mass stratification that allowed faster sedimentation of the relatively light *T. quinqueloba* tests (Schiebel and Hemleben, 2017). These changes may have been related to changes in the AF. Interestingly, SIMMAX reconstructions from the Mediterranean Sea (Sicre et al., 2013) show cold SST_{su} estimates similar to our coring site, also being associated to abundance peaks of *T. quinqueloba*.

Enhanced abundances *G. scitula* indicate a southward displacement of the AF from interglacial to glacial conditions and suggest that the abundance changes were caused by changes in the latitudinal position of the frontal systems of the subtropical NA (Schiebel et al., 2002a). Consequently, oscillations of the AF between more southward and northward positions could explain the frequent changes in SIMMAX SST.

Despite the likelihood that the extreme cooling in the SIMMAX record was caused by a strong imprint of the assemblage change, in the following the plausibility of the amplitude of SST change is tested. For this purpose, we use the assumption that the northern limit of the STG was displaced southward during the deglacial cold H1 and IACP events (Repschläger et al., 2015). Further, we assume that the high relative abundances of *G. scitula* during IACP were associated with the presence of temperate to subpolar waters at the coring site. The latter might even be coupled with an extreme southward displacement of the Arctic Front (e.g., Bard et al., 1987; Eynaud et al., 2009, and citations therein). These events were most probably caused by massive meltwater outbursts from the Laurentian ice sheets that penetrated the NA (e.g., Obbink et al., 2010).

Assuming that subpolar conditions prevailed at the Azores coring site during cold events, coldest possible SSTs would match

SSTs observed in the northern NA. Mg/Ca SSTs derived from *G. bulloides* and *N. pachyderma* from the subpolar NA (52 to 62°N) indicate a cooling by 7–8°C from 11–15°C down to 6–7°C for the IACP and YD (Came et al., 2007; Peck et al., 2008; Benway et al., 2010; Thornalley et al., 2010) and SIMMAX SST reconstructions indicate that summer SSTs cooled down by 7°C from 15°C to 8°C at 50°N (site BOFS 5K) after BA (Maslin et al., 1995). During H1, it was even colder with SIMMAX-derived SST_{su} of 3°C at 50°N (Maslin et al., 1995), 7°C according to MAT, 9–10°C according to U^{K'}₃₇ SST (Pérez-Folgado et al., 2003) and 10°C (MAT) at 40°N (Chapman et al., 2000). Within all of these records, SIMMAX SST_{su} indicate the strongest cooling and might be overprinted by water mass changes due to frontal movements as supposed at the AF.

All of these reconstructions show that during H1 and IACP SSTs in the subpolar North Atlantic are even lower than our SIMMAX SST_{su} of 10°C close to the AF. A southward extension of this water mass could be a potential source for the extreme cooling signals.

In order to comprehensively address the potential cooling signal, we also test the feasibility of the SST estimates for sub-millennial scale cold events by comparing our result with those of climate simulations. In several coupled ocean atmosphere model experiments with a freshwater induced AMOC collapse, SSTs cool down by up to 13°C in the subpolar region, whereas the cooling outside of the subpolar region does not exceed 5°C (Stouffer et al., 2006; Liu et al., 2009; Kageyama et al., 2010). Within the uncertainty of the models a 4–6°C cooling at the Azores coring site is reasonable, but seems to be highly dependent on the position of the AF. This highlights the importance of a reliable and detailed reconstruction in paleoceanography and ocean circulation models.

Similar absolute temperatures of 10–12°C are observed in the SIMMAX reconstructions (Figure 2A) during the two major cold events (H1 and IACP). This scenario is unlikely because of the different climatic background conditions before, during, and after the deglacial warming and ice sheet melting. SST signals of this amplitude are neither observed in the subpolar nor polar NA. This cooling is also not supported by the other SST reconstructions at the Azores coring site. Therefore, we assume that temperature amplitudes of up to 12°C as estimated for the IACP cooling when using SIMMAX SST reconstructions at the Azores coring site are overestimated.

5.4. Younger dryas subsurface influence on the SIMMAX SST record

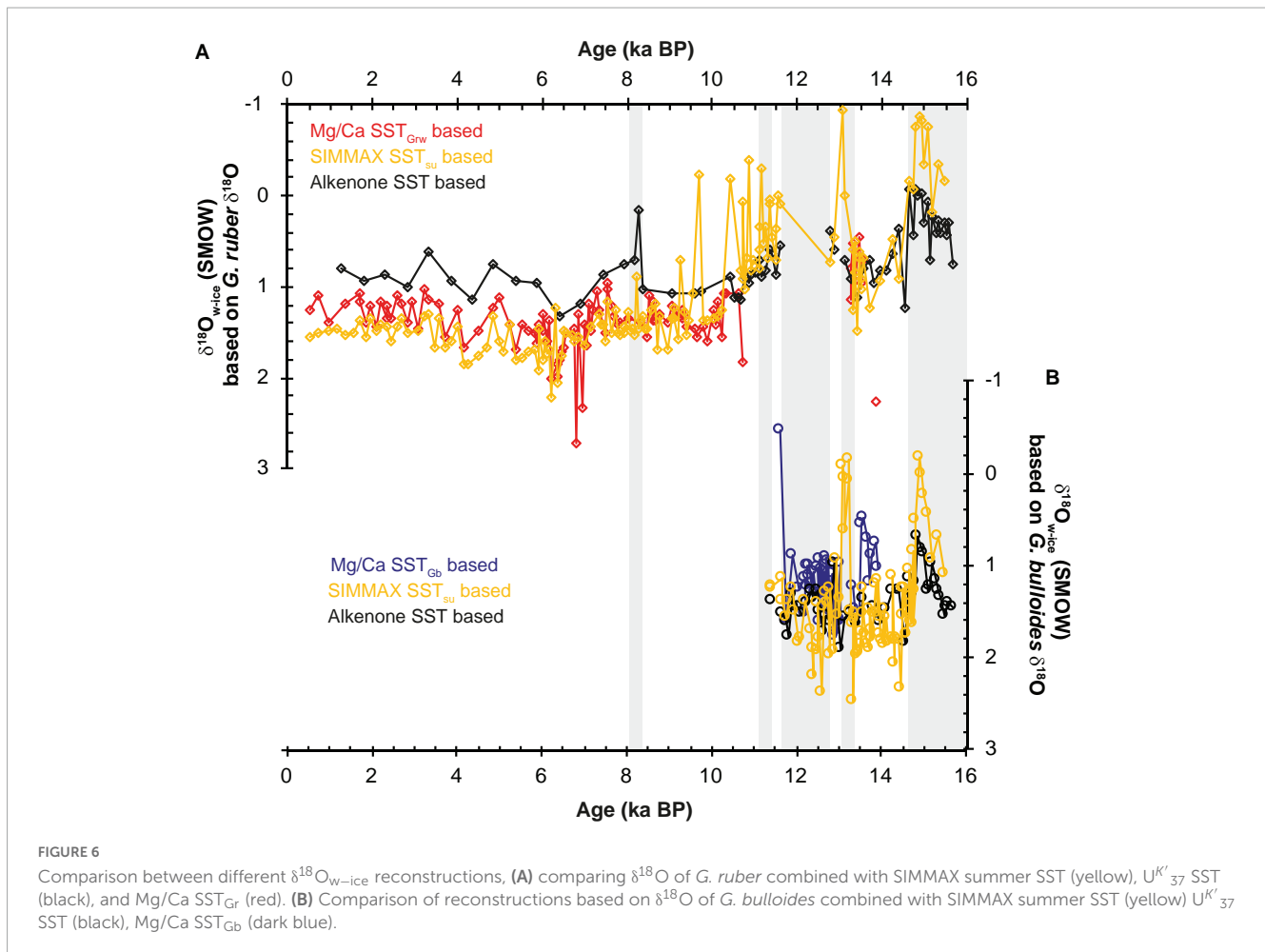
The SIMMAX, U^{K'}₃₇ SST, and Mg/Ca SST_{Gb} signals are decoupled during the YD (Figure 2D). SIMMAX SSTs suggest a short-term warming event shortly after the beginning of the YD cooling, while U^{K'}₃₇ SSTs and Mg/Ca SST_{Gb} decrease down to 15°C at the onset of the YD, and remain at 15–16°C (Figure 1C) similar to Mg/Ca T_{Gtrunc} subsurface temperatures. Thus, either U^{K'}₃₇ reconstructions do not correctly account for this relatively short warming interval, or YD-cooling is masked in the SIMMAX SST record. SIMMAX SSTs may also reflect subsurface SSTs rather than sea surface conditions during cold excursions due to high relative abundances of subsurface dwelling foraminifers as suggested by Telford et al. (2013).

A strong impact of the temperate surface-dwelling species *N. incompta* (Schiebel and Hemleben, 2000; Schiebel et al., 2002a; Rebotim et al., 2017) on the SIMMAX SST_{su} record becomes most evident in the close match between the SIMMAX SST record and the inverse record of *N. incompta* abundance (Figure 5). This record shows an increasing abundance of *N. incompta* during the cold YD, whereas the subtropical *G. ruber* become rare, <4% (Figure 3A). Thus, *N. incompta* becomes one of the dominant species during the YD and its abundance pattern becomes similar to the pattern of the SIMMAX SST record (Figure 5). During this time-period, stratification of the surface water column was different from the modern, and a stronger increase of subsurface than shallow-dwelling species probably led to an increased effect of subsurface conditions on the SST reconstruction. Thus, SIMMAX SST cannot exclusively be regarded as a surface water signal in this part of the YD record given the complex hydrological situation at the AF. As soon as the *G. ruber* population recovers in the MH, SIMMAX SSTs seem to reflect surface temperatures again.

U^{K'}₃₇ SST similar to Mg/Ca SST_{Gb} during YD, again can be explained by similar seasonality and dwelling depths of the alkenone producing coccolithophores and *G. bulloides*. Similar Mg/Ca SST_{Gb}, U^{K'}₃₇ SST and Mg/Ca SST_{Gtrunc} may relate to subsurface warming (Repschläger et al., 2015), to a collapse of the winter stratification or to yet unknown changes in the life cycle of *G. truncatulinoides*.

5.5. Comparison of the minor cooling during EH “flickering” phase with deglacial cold events

A series of minor cold-warm oscillations are evident within the SIMMAX SST record during the EH (Figure 2A). These results are not reproduced when using the combined Atlantic and Mediterranean dataset and indicate, that the “flickering” is caused by non-analog situations in the calibration dataset. Yet, the cold events within these oscillations cannot be related to an increase in frequency of the cold-water species *G. scitula* and *T. quinqueloba* (Figures 3C, F), as during H1 and IACP. This “flickering” temperature signal in the SIMMAX SST record in the EH might result from minor changes in the faunal assemblage that are related to changes in the position and structure of the AF. These changes are a combination of strongly varying *G. bulloides* and *G. glutinata* abundances, and slowly increasing *G. ruber* and decreasing *N. incompta* abundances. Due to underrepresentation of AF assemblages (Storz et al., 2009) in the calibration dataset, these minor compositional changes might lead to a pronounced switch of the SIMMAX SST based either on subpolar or transitional samples on the SST reconstruction. Interestingly, the cold events match the periods of several subordinate meltwater pulses of the Laurentian Ice sheet draining the St. Lawrence River (Teller et al., 2002; Jennings et al., 2015). Therefore, these waters may have had a less strong impact on the STG than the main meltwater drainage events during H1, IACP, and 8.2-ka-BP-Event (Repschläger et al., 2015) that are related to meltwater pulses from Hudson Bay (Teller et al., 2002). This assumption still needs to be tested with independent high-resolution δ¹⁸O_w reconstructions by combined



Mg/Ca SST and $\delta^{18}\text{O}$ measurements. The change in the *G. bulloides* vs. *G. glutinata* abundance might be associated with a change in the seasonal succession of species, potentially associated with a higher tolerance of *G. glutinata* to lower SST. Alternatively, *G. bulloides* might lack one of the main abundance peaks in autumn, but which more typically occurs further north (Jonkers and Kučera, 2015).

5.6. Effect of SST on derived local $\delta^{18}\text{O}_{sw}$ reconstructions

In the following, we assess the effect of the combination of temperature reconstructions with $\delta^{18}\text{O}$ measurements from different proxies to assess $\delta^{18}\text{O}_{w-ice}$ changes at our core site. $\delta^{18}\text{O}_{w-ice}$ was calculated from the temperature reconstructions from Mg/Ca SST_{Gr}, Mg/Ca SST_{Gb}, $U^{K'}_{37}$ SST and SIMMAX SST_{su}, in combination with $\delta^{18}\text{O}$ records from surface dwelling *G. bulloides* and *G. ruber* (Figure 6). Given the offsets in SST reconstructions revealed by our multiproxy study, the combination of temperature reconstructions from different proxy-bearing organisms with $\delta^{18}\text{O}$ measurements can have a severe effect on calculated $\delta^{18}\text{O}_{w-ice}$ records. In general, SIMMAX based $\delta^{18}\text{O}_{w-ice}$ records are more variable than other records and reflect the variability of SIMMAX SST records. The *G. ruber* $\delta^{18}\text{O}$ and Mg/Ca

SST_{Gr} based $\delta^{18}\text{O}_{w-ice}$ reconstructions are similar to those based on SIMMAX SST_{su} during the Holocene (Figure 6A), while the *G. ruber* $\delta^{18}\text{O}$ and $U^{K'}_{37}$ based records are systematically lower in $\delta^{18}\text{O}_{w-ice}$ values. For the YD and BA records based on *G. bulloides* $\delta^{18}\text{O}$, Mg/Ca SST_{Gr}, Mg/Ca SST_{Gb}, and $U^{K'}_{37}$ (Figure 6B) are in good agreement with exception of short-term freshening events coinciding with the extreme cooling events in the SIMMAX record.

The average differences between the $U^{K'}_{37}$ and SIMMAX based reconstructions amount to 0.5 ‰ SMOW in the Holocene. This difference can be regarded as an estimate for the imprint that seasonality can cause on the $\delta^{18}\text{O}_{w-ice}$ signal. Results of SIMMAX based reconstructions indicate a strong freshening of 2 ‰ SMOW during cold H1 and 8.2-ka-BP-Event, whereas freshening amounts to 1 ‰ SMOW in all other reconstructions. Hence, the too cold SIMMAX SSTs during these intervals lead to an overestimation of the freshening by 1 ‰ SMOW. These results show that differences in the productive seasons of the different organisms carrying the SST or $\delta^{18}\text{O}$ signals may result in differences in calculated $\delta^{18}\text{O}_{w-ice}$ at the same order of magnitude as a signal of seawater freshening itself. Therefore, it is important to combine $\delta^{18}\text{O}$ signals and SST signals for $\delta^{18}\text{O}_{w-ice}$ reconstructions representative of the same season and dwelling depth, ideally together with Mg/Ca temperatures and $\delta^{18}\text{O}$ reconstructions from the same planktic foraminifer sample.

5.7. Reconstruction of seasonal differences using a multiproxy approach

Changes in the phenology of coccolithophores and planktic foraminifers in the North Atlantic are a matter of changes in the growth period (Hopkins et al., 2015; Kretschmer et al., 2018). However, little is known about seasonal changes, i.e., onset and duration of seasons on longer time scales such as glacial-interglacial cycles, although seasonality might have a major impact on and might be impacted by climate variability. Under the assumption that different species of planktic foraminifers and coccolithophores produce Mg/Ca and alkenones signals during different seasons in the North Atlantic, these differences could be used in a combined approach to reconstruct temperature changes between spring, summer, and autumn. The difference between average Mg/Ca SST_{Gr} (summer SST) and U^{K'}₃₇ (spring SST) increases from 2.3°C during BA to 2.7°C and 2.9°C over the Early and Late Holocene, respectively. The latter increase (BA to Late Holocene) in SST difference may relate to an increase in absolute seasonal differences in SST between BA and Late Holocene. In addition, extremely cold winter temperatures are proposed for the YD interval (Denton et al., 2005). Colder than modern winters might also have prevailed during BA and may have led to a shift of the growth periods of different species to different degrees. Consequently, the spring bloom may have been delayed while summer conditions were possibly constant during peak summer SST.

6. Conclusion

Distinct differences in multiproxy SST records are caused by the unique nature of the different archives and are influenced by the ecology of the proxy bearing organisms, including depth habitat and main growing season. Once understood, these differences may help to better reconstruct changes in seasonal temperature and surface ocean stratification, which are major unknowns in global climate reconstruction.

In order to better understand the different imprints on the SST proxies in the North Atlantic, a multiproxy SST record from the boundary between the subtropical and the temperate North Atlantic was analyzed and discussed under consideration of the phenology and habitat depth of different paleoceanographic proxies. The comparison between the SST indicates that the different temperature proxies of planktic foraminifer based transfer calculations (SIMMAX), Mg/Ca of different planktic foraminifer species, and alkenones do not only record changes in annual temperatures but also give an insight into changes in different seasonal temperatures. The main findings are that

- Mg/Ca SST reconstructions from *G. ruber* are similar in the BA and Holocene, and most likely reflect summer SSTs down to 50 m water depth at the northern edge of the subtropical gyre.
- Mg/Ca SST reconstructions from *G. bulloides* mainly reflect temperatures of the upper 60 to 100 m water depth in spring, and, thereby, in the same season as the alkenones.
- Mg/Ca T reconstructions from *G. truncatulinoides* reflect temperatures at thermocline depth (100–150 m) that are

decoupled from the sea surface and indicate subsurface warming during BA and YD period.

- U^{K'}₃₇ SST reflect surface water temperatures in the upper 50 m during late spring and show the well-known deglacial North Atlantic succession of warm and cold events. U^{K'}₃₇ SST may underestimate the overall deglacial temperature amplitudes and the magnitude of short-term cooling events (e.g., H1, IACP, and 8.2-ka-BP-Event) that interrupt the long-term deglacial and Holocene SST evolution due to changes in phenology.
- Faunal assemblage changes seem to record water mass changes, even in situations of minor SST changes, which are not unequivocally displayed by SIMMAX SST reconstructions. Thus, SIMMAX SSTs using the original calibration dataset (Pflaumann et al., 1996) are more sensitive to changes in water mass distribution rather than changes in the absolute SST, and result in over- or underestimation of SST changes. These differences become greater at strong SIMMAX SST cooling during the two major cold events H1 and IACP, and minor cold oscillations during the Early Holocene. An overestimation of SSTs during the early YD is probably caused by SIMMAX SSTs reflecting subsurface conditions that indicate thermocline warming.
- Despite methodological differences, strong cooling at the core site SW of the Azores during the major cold events H1 and IACP is indicated by the occurrence of subpolar faunal elements.
- Differences between U^{K'}₃₇ SST and Mg/Ca SST_{Gr} reconstructions could be used to assess changes in duration and/or amplitude of seasonal changes in our study region.
- Ecological differences resulting from seasonality and dwelling depth in the chosen SST signals can have strong effects on δ¹⁸O_{w-ice} reconstructions, probably of an amount similar to the effects of freshening events.

Data availability statement

The original contributions presented in this study are included in the article/[Supplementary material](#), further inquiries can be directed to the corresponding author.

Author contributions

JR, RalphS, and MW contributed to conception and design of the study. JR and MW performed the faunal assemblage counting and SIMMAX calculations. JR analyzed the data wrote the first draft of the manuscript. All authors contributed to manuscript revision, read, and approved the submitted version.

Funding

Publication of this manuscript has been supported by the European Science Foundation (ESF) under the EUROCORES Program EuroMARC, ERASCT-2003-980409 of the European Commission, DG Research, FPG. Financial support was provided by the German Research Foundation (DFG grant number WE 2679/6-1).

Acknowledgments

The results represented here are obtained from cores taken on board the R/V Marion Dufresne (French Polar Institute, IPEV) during the IMAGES-AMOCINT MD168-cruise in the framework of the 06-EuroMARC-FP-006 Project. We thank the captain and crew, as well as our colleagues on board for their help. Furthermore, we also thank Bernard Dennielou and IFREMER for providing us with material from core GEOFAR KF16.

Conflict of interest

The authors declare that the research was conducted in the absence of any commercial or financial relationships that could be construed as a potential conflict of interest.

References

- Adloff, F., Mikolajewicz, U., Kučera, M., Grimm, R., Maier-Reimer, E., Schmiedel, G., et al. (2011). Upper ocean climate of the eastern Mediterranean sea during the Holocene insolation maximum—A model study. *Clim. Past* 7, 1103–1122. doi: 10.5194/cp-7-1103-2011
- Alves, M., Gaillard, F., Sparrow, M., Knoll, M., and Giraud, S. (2002). Circulation patterns and transport of the Azores front-current system. *Deep Sea Res. Part II* 49, 3983–4002. doi: 10.1016/S0967-0645(02)00138-8
- Anand, P., Elderfield, H., and Conte, M. H. (2003). Calibration of Mg/Ca thermometry in planktonic foraminifera from a sediment trap time series. *Paleoceanography* 18:1050. doi: 10.1029/2002PA000846
- Andersen, K. K., Svensson, A., Rasmussen, S. O., Steffensen, J. P., Johnsen, S. J., Bigler, M., et al. (2006). The Greenland ice core chronology 2005, 150-0 ka. Part 1: Constructing the time scale. *Quat. Sci. Rev.* 25, 3246–3257. doi: 10.1016/j.quascirev.2006.08.002
- Annan, J. D., and Hargreaves, J. C. (2013). A new global reconstruction of temperature changes at the last glacial maximum. *Clim. Past* 9, 367–376. doi: 10.5194/cp-9-367-2013
- Arbuszewski, J., deMenocal, P., Kaplan, A., and Farmer, E. C. (2010). On the fidelity of shell-derived $\delta^{18}\text{O}_{\text{seawater}}$ estimates. *Earth Planet. Sci. Lett.* 300, 185–196. doi: 10.1016/j.epsl.2010.10.035
- Austermann, J., Mitrovica, J. X., Latychev, K., and Milne, G. (2013). Barbados-based estimate of ice volume at last glacial maximum affected by subducted plate. *Nat. Geosci.* 6, 553–557. doi: 10.1038/ngeo1859
- Balmer, S., and Sarntheim, M. (2018). Glacial-to-deglacial changes in North Atlantic meltwater advection and deep-water formation—Centennial-to-millennial-scale 14C records from the Azores plateau. *Geochim. Cosmochim. Acta* 236, 399–415. doi: 10.1016/j.gca.2018.03.001
- Bard, E. (2001a). Comparison of alkenone estimates with other paleotemperature proxies. *Geochem. Geophys. Geosyst.* 2, 1002–1012. doi: 10.1029/2000GC000050
- Bard, E. (2001b). Paleoceanographic implications of the difference in deep-sea sediment mixing between large and fine particles. *Paleoceanography* 16, 235–239. doi: 10.1029/2000PA000537
- Bard, E., Arnold, M., Maurice, P., Duprat, J., Moyes, J., and Duplessy, J. (1987). Retreat velocity of the North Atlantic polar front during the last deglaciation determined by 14C accelerator mass spectrometry. *Nature* 328, 791–794. doi: 10.1038/328791a0
- Barker, S., Greaves, M., and Elderfield, H. (2003). A study of cleaning procedures used for foraminiferal Mg/Ca paleothermometry. *Geochem. Geophys. Geosyst.* 4:8407. doi: 10.1029/2003GC000559
- Bé, A. W. H., and Tolderlund, D. S. (1971). “Distribution and ecology of living planktonic foraminifera in surface waters of the Atlantic and Indian oceans,” in *Micropaleontology of the oceans*, eds B. M. Funnell and W. R. Riedel (London: Cambridge University Press), 105–149.
- Benway, H., McManus, J., Oppo, D., and Cullen, J. (2010). Hydrographic changes in the eastern subpolar North Atlantic during the last deglaciation. *Quat. Sci. Rev.* 29, 3336–3345. doi: 10.1016/j.quascirev.2010.12.014
- Berger, A., and Loutre, M. (1991). Insolation values for the climate of the last 10 million years. *Quat. Sci. Rev.* 10, 297–317. doi: 10.1016/0277-3791(91)90033-Q
- Bian, N., and Martin, P. (2010). Investigating the fidelity of Mg/Ca and other elemental data from reductively cleaned planktonic foraminifera. *Paleoceanography* 25:A2215. doi: 10.1029/2009pa001796
- Bradshaw, J. (1957). Ecology of living planktonic foraminifera in the north and equatorial Pacific ocean. *Cushman Found. Foramin. Res. Contrib.* 10, 25–64.
- Came, R., Oppo, D., and McManus, J. (2007). Amplitude and timing of temperature and salinity variability in the subpolar North Atlantic over the past 10 k.y. *Geology* 35, 315–318. doi: 10.1130/g23455a.1
- Chapman, M. (2010). Seasonal production patterns of planktonic foraminifera in the NE Atlantic ocean: Implications for paleotemperature and hydrographic reconstructions. *Paleoceanography* 25:A1101. doi: 10.1029/2008PA001708
- Chapman, M. R., Shackleton, N. J., Zhao, M., and Eglinton, G. (1996). Faunal and alkenone reconstructions of subtropical North Atlantic surface hydrography and paleotemperature over the last 28 kyr. *Paleoceanography* 11, 343–357. doi: 10.1029/96PA00041
- Chapman, M., Shackleton, N., and Duplessy, J. (2000). Sea surface temperature variability during the last glacial-interglacial cycle: Assessing the magnitude and pattern of climatic change in the North Atlantic. *Paleogeogr. Paleoclimatol. Paleoecol.* 157, 1–25.
- Cléroux, C., Cortijo, E., Anand, P., Labeyrie, L. D., Bassinot, F., Caillon, N., et al. (2008). Mg/Ca and Sr/Ca ratios in planktonic foraminifera: Proxies for upper water column temperature reconstruction. *Paleoceanography* 23:A3214. doi: 10.1029/2007PA001505
- Cléroux, C., Cortijo, E., Duplessy, J., and Zahn, R. (2007). Deep-dwelling foraminifera as thermocline temperature recorders. *Geochem. Geophys. Geosyst.* 8:Q04N11. doi: 10.1029/2006GC001474
- CLIMAP Project Members (1981). Seasonal reconstruction of the earth's surface at the last glacial maximum. *Geol. Soc. Am. Map Chart Series* 36:18.
- DeKens, P. S., Lea, D. W., Pak, D. K., and Spero, H. J. (2002). Core top calibration of Mg/Ca in tropical foraminifera: Refining paleotemperature estimation. *Geochem. Geophys. Geosystems* 3, 1–29. doi: 10.1029/2001GC000200
- Denton, G. H., Alley, R. B., Comer, G. C., and Broecker, W. S. (2005). The role of seasonality in abrupt climate change. *Quat. Sci. Rev.* 24, 1159–1182. doi: 10.1016/j.quascirev.2004.12.002
- Duplessy, J. C., Labeyrie, L. D., Juillet-Leclerc, A., Maitre, F., Duprat, J. M., and Sarntheim, M. (1991). Surface salinity reconstruction of the North Atlantic ocean during the last glacial maximum. *Oceanol. Acta* 14, 311–324.
- Elderfield, H., and Ganssen, G. (2000). Past temperature and $\delta^{18}\text{O}$ of surface ocean waters inferred from foraminiferal Mg/Ca ratios. *Nature* 405, 442–445. doi: 10.1038/35013033
- Evans, D., Wade, B. S., Henahan, M., Erez, J., and Müller, W. (2016). Revisiting carbonate chemistry controls on planktic foraminifera Mg/Ca: Implications for sea surface temperature and hydrology shifts over the paleocene-eocene thermal

Publisher's note

All claims expressed in this article are solely those of the authors and do not necessarily represent those of their affiliated organizations, or those of the publisher, the editors and the reviewers. Any product that may be evaluated in this article, or claim that may be made by its manufacturer, is not guaranteed or endorsed by the publisher.

Supplementary material

The Supplementary Material for this article can be found online at: <https://www.frontiersin.org/articles/10.3389/fevo.2023.1176278/full#supplementary-material>

- maximum and eocene–oligocene transition. *Clim. Past* 12, 819–835. doi: 10.5194/cp-12-819-2016
- Eynaud, F., de Abreu, L., Voelker, A. H., Schönfeld, J., Salgueiro, E., Turon, J. L., et al. (2009). Position of the polar front along the western Iberian margin during key cold episodes of the last 45 ka. *Geochim. Geophys. Geosystems*. 10:Q07U05. doi: 10.1029/2009GC002398
- Frailé, I., Schulz, M., Mulitza, S., Merkel, U., Prange, M., and Paul, A. N. (2009). Modeling the seasonal distribution of planktonic foraminifera during the last glacial maximum. *Paleoceanography* 24:A2216. doi: 10.1029/2008PA001686
- Friedrich, O., Schiebel, R., Wilson, P., Weldeab, S., Beer, C., Cooper, M., et al. (2012). Influence of test size, water depth, and ecology on Mg/Ca, Sr/Ca, $\delta^{18}O$ and $\delta^{13}C$ in nine modern species of planktic foraminifers. *Earth Planet. Sci. Lett.* 320, 133–145. doi: 10.1016/j.epsl.2011.12.002
- Gould, W. (1985). Physical oceanography of the Azores front. *Prog. Oceanogr.* 14, 167–190. doi: 10.1098/rspb.2010.0900
- Gray, W., and Evans, D. (2019). Nonthermal influences on Mg/Ca in planktonic foraminifera: A review of culture studies and application to the last glacial maximum. *Paleoceanogr. Paleoclimatol.* 34, 306–315. doi: 10.1029/2018PA003517
- Gray, W., Weldeab, S., Lea, D., Rosenthal, Y., Gruber, N., Donner, B., et al. (2018). The effects of temperature, salinity, and the carbonate system on Mg/Ca in *Globigerinoides ruber* (white): A global sediment trap calibration. *Earth Planet. Sci. Lett.* 482, 607–620. doi: 10.1016/j.epsl.2017.11.026
- Haidar, A. T., and Thierstein, H. R. (2001). Coccolithophore dynamics off Bermuda (N. Atlantic). *Deep Sea Res. Part II* 48, 1925–1956. doi: 10.1016/S0967-0645(00)0169-7
- Hemleben, C., Spindler, M., and Anderson, O. R. (1989). *Modern planktonic foraminifera*. Berlin: Springer, 363.
- Henson, S. A., Dunne, J. P., and Sarmiento, J. L. (2009). Decadal variability in North Atlantic phytoplankton blooms. *J. Geophys. Res.* 114:C04013. doi: 10.1029/2008JC005139
- Hertzberg, J. E., and Schmidt, M. W. (2013). Refining *Globigerinoides ruber* Mg/Ca paleothermometry in the Atlantic ocean. *Earth Planet. Sci. Lett.* 383, 123–133. doi: 10.1016/j.epsl.2013.09.044
- Hessler, I., Harrison, S. P., Kucera, M., Waelbroeck, C., Chen, M.-T., Anderson, C., et al. (2014). Implication of methodological uncertainties for mid-Holocene sea surface temperature reconstructions. *Clim. Past* 10, 2237–2252. doi: 10.5194/cp-10-2237-2014
- Hopkins, J., Henson, S. A., Painter, S. C., Tyrrell, T., and Poulton, A. J. (2015). Phenological characteristics of global coccolithophore blooms. *Glob. Biogeochem. Cycles* 29, 239–253. doi: 10.1002/2014GB004919
- Husum, K., and Hald, M. (2012). Arctic planktic foraminiferal assemblages: Implications for subsurface temperature reconstructions. *Mar. Micropaleontol.* 96–97, 38–47. doi: 10.1016/j.marmicro.2012.07.001
- Huybers, P., and Curry, W. (2006). Links between annual, milankovitch and continuum temperature variability. *Nature* 441, 329–332. doi: 10.1038/nature04745
- Jansen, E., Andersson, C., Moros, M., Nisancioglu, K. H., Nyland, B. F., and Telford, R. J. (2009). “The early to mid-holocene thermal optimum in the north Atlantic,” in *Natural climate variability and global warming*, eds R. W. Battarbee and H. A. Binney (Hoboken, NJ: Wiley Blackwell), 123–137.
- Jennings, A., Andrews, J., Pearce, C., Wilson, L., and Olfadottir, S. (2015). Detrital carbonate peaks on the Labrador shelf, a 13–7 ka template for freshwater forcing from the Hudson Strait outlet of the Laurentide ice sheet into the subpolar gyre. *Quat. Sci. Rev.* 107, 62–80. doi: 10.1016/j.quascirev.2014.10.022
- Jentzen, A., Nürnberg, D., Hathorne, E., and Schönfeld, J. (2018). Mg/Ca and $\delta^{18}O$ in living Planktic foraminifers from the Caribbean, gulf of Mexico and Florida straits. *Biogeosciences* 15, 7077–7095. doi: 10.5194/bg-15-7077-2018
- Johannessen, T., Jansen, E., Flatoy, A., and Ravelo, A. C. (1994). “The relationship between surface water masses, oceanographic fronts and paleoclimatic proxies in surface sediments of the Greenland, Iceland, Norwegian Seas,” in *Paper presented at the carbon cycling in the glacial ocean: Constraints on the ocean’s role in global change*, (Berlin: Springer), 61–85. doi: 10.1007/978-3-642-78737-9_4
- Jonkers, L., and Kucera, M. (2015). Global analysis of seasonality in the shell flux of extant planktonic foraminifera. *Biogeosciences* 12, 2207–2226. doi: 10.5194/bg-12-2207-2015
- Jonkers, L., Brummer, G.-J. A., Peeters, F. J. C., van Aken, H. M., and De Jong, M. F. (2010). Seasonal stratification, shell flux, and oxygen isotope dynamics of left-coiling *N. pachyderma* and *T. quinqueloba* in the western subpolar north Atlantic. *Paleoceanography* 25:A2204. doi:10.1029/2009pa001849
- Jonkers, L., van Heuven, S., Zahn, R., and Peeters, F. J. C. (2013). Seasonal patterns of shell flux, $\delta^{18}O$ and $\delta^{13}C$ of small and large *N. pachyderma* (s) and *G. bulloides* in the subpolar north Atlantic. *Paleoceanography* 28, 164–174. doi:10.1002/palo.20018
- Kageyama, M., Paul, A., Roche, D., and Van Meerbeek, C. (2010). Modelling glacial climatic millennial-scale variability related to changes in the Atlantic meridional overturning circulation: A review. *Quat. Sci. Rev.* 29, 2931–2956.
- Käse, R. H., and Siedler, G. (1982). Meandering of the subtropical front south-east of the Azores. *Nature* 300, 245–246.
- Kisakürek, B., Eisenhauer, A., Böhm, F., Garbe-Schönberg, D., and Erez, J. (2008). Controls on shell Mg/Ca and Sr/Ca in cultured planktonic foraminifera, *Globigerinoides ruber* (white). *Earth Planet. Sci. Lett.* 273, 260–269. doi: 10.1016/j.epsl.2008.06.026
- Kissel, C., Kleiven, H., and Morin, X. (2008). “The shipboard scientific party. MD168-AMOCINT/XVII IMAGES cruise report,” in *Les rapports de campagne à la mer, IPEV, ref: OCE/2008/02*, 5.
- Kozdon, R., Eisenhauer, A., Weinelt, M., Meland, M., and Nuernberg, D. (2009). Reassessing Mg/Ca temperature calibrations of *Neogloboquadrina pachyderma* (sinistral) using paired $\delta^{44}Ca/^{40}Ca$ and Mg/Ca measurements. *Geochim. Geophys. Geosystems*. 10:Q03005. doi: 10.1029/2008gc002169
- Kretschmer, K., Jonkers, L., Kucera, M., and Schulz, M. (2018). Modeling seasonal and vertical habitats of planktonic foraminifera on a global scale. *Biogeosciences* 15, 4405–4429. doi: 10.5194/bg-15-4405-2018
- Kretschmer, K., Kucera, M., and Schulz, M. (2016). Modeling the distribution and seasonality of *Neogloboquadrina pachyderma* in the north Atlantic ocean during heinrich stadial 1. *Paleoceanography* 31, 986–1010. doi: 10.1002/2015PA002819
- Kucera, M., Rosell-Melé, A., Schneider, R., Waelbroeck, C., and Weinelt, M. (2005). Multiproxy approach for the reconstruction of the glacial ocean surface (MARGO). *Quat. Sci. Rev.* 24, 813–819. doi: 10.1016/j.quascirev.2004.07.017
- Laepple, T., and Huybers, P. (2014). Ocean surface temperature variability: Large model–data differences at decadal and longer periods. *Proc. Natl. Acad. Sci. U.S.A.* 111:16682. doi: 10.1073/pnas.1412077111
- Lea, D., Pak, D., and Spero, H. (2000). Climate impact of late quaternary equatorial Pacific sea surface temperature variations. *Science* 289, 1719–1724. doi: 10.1126/science.289.5485.1719
- Leduc, G., de Garidel-Thoron, T., Kaiser, J., Bolton, C., and Contoux, C. (2017). Databases for sea surface paleotemperature based on geochemical proxies from marine sediments: Implications for model-data comparisons. *Quaternaire* 28, 201–216. doi: 10.4000/quaternaire.8034
- Leduc, G., Garbe-Schönberg, D., Regenberg, M., Contoux, C., Etourneau, J., and Schneider, R. (2014). The late pliocene benguela upwelling status revisited by means of multiple temperature proxies. *Geochim. Geophys. Geosystems*. 15, 475–491. doi: 10.1002/2013GC004940
- Leduc, G., Schneider, R. R., Kim, J., and Lohmann, G. (2010). Holocene and Eemian sea surface temperature trends as revealed by alkenone and Mg/Ca paleothermometry. *Quat. Sci. Rev.* 29, 989–1004.
- Levitus, S., and Boyer, T. P. (1994). *World ocean atlas. NOAA atlas DIS*. Washington, DC: U.S. Government Printing Office, 117.
- Liu, M., and Tanhua, T. (2019a). Characteristics of water masses in the Atlantic ocean based on GLODAPv2 data. *Ocean Sci. Discuss.* 2019, 1–43. doi: 10.5194/os-2018-139
- Liu, M., and Tanhua, T. (2019b). Distribution of water masses in the Atlantic ocean based on GLODAPv2. *Ocean Sci. Discuss.* 2019, 1–32. doi: 10.5194/os-2018-140
- Liu, Z., Otto-Bliessner, B., He, F., Brady, E., Tomas, R., Clark, P., et al. (2009). Transient simulation of last deglaciation with a new mechanism for boling-allered warming. *Science* 325, 310–314. doi: 10.1126/science.1171041
- Locarnini, R. A., Mishonov, A. V., Antonov, J. I., Boyer, T. P., Garcia, H. E., Baranova, O. K., et al. (2013). *World ocean atlas 2013, temperature*, NOAA Atlas NESDIS, ed. S. Levitus, A. Mishonov Technical Edn, 73, Vol. 1, 40.
- Lohmann, G., Pfeiffer, M., Laepple, T., Leduc, G., and Kim, J.-H. (2012). A model-data comparison of the holocene global sea surface temperature evolution. *Clim. Past Discuss.* 8, 1005–1056. doi: 10.5194/cpd-8-1005-2012
- Lombard, F., Labeyrie, L. D., Michel, E., Bopp, L., Cortijo, E., Retaillieu, S., et al. (2011). Modelling planktic foraminifer growth and distribution using an ecophysiological multi-species approach. *Biogeosciences* 8, 853–873.
- Longhurst, A. (2007). *Ecological geography of the sea*. Amsterdam: Academic Press.
- MARGO Project Members (2009). Constraints on the magnitude and patterns of ocean cooling at the last glacial maximum. *Nat. Geosci.* 2, 127–132. doi: 10.1038/ngeo411
- Maslin, M. A., Shackleton, N. J., and Pflaumann, U. (1995). Surface water temperature, salinity, and density changes in the northeast Atlantic during the last 45,000 years: Heinrich events, deep water formation, and climatic rebounds. *Paleoceanography* 10, 527–544. doi: 10.1029/94pa03040
- Mason, S., and Oliveira, P. (2006). An overview of the literature concerning the oceanography of the eastern north Atlantic region. *Relat. Cient. Tec. IPIMAR Serie Digit.* 33:58.
- Mathien-Blard, E., and Bassinot, F. (2009). Salinity bias on the foraminifera Mg/Ca thermometry: Correction procedure and implications for past ocean hydrographic reconstructions. *Geochim. Geophys. Geosystems*. 10:Q12011. doi: 10.1029/2008gc002353

- McCartney, M. S., and Talley, L. D. (1982). The subpolar mode water of the north Atlantic ocean. *J. Phys. Oceanogr.* 12, 1169–1188. doi: 10.1175/1520-04851982012<1169:TSMWOT>2.0.CO;2
- McConnell, M. C., and Thunell, R. C. (2005). Calibration of the planktonic foraminiferal Mg/Ca paleothermometer: Sediment trap results from the guaymas basin, gulf of California. *Paleoceanography* 20:A2016. doi: 10.1029/2004PA001077
- McConnell, M. C., Thunell, R. C., Lorenzoni, L., Astor, Y., Wright, J. D., and Fairbanks, R. (2009). Seasonal variability in the salinity and oxygen isotopic composition of seawater from the Cariaco basin, Venezuela: Implications for paleosalinity reconstructions. *Geochem. Geophys. Geosystems*. 10:Q06019. doi: 10.1029/2008GC002035
- Meland, M. Y., Jansen, E., and Elderfield, H. (2005). Constraints on SST estimates for the northern North Atlantic/Nordic Seas during the LGM. *Quat. Sci. Rev.* 24, 835–852.
- Mollenhauer, G., Kienast, M., Lamy, F., Meggers, H., Schneider, R. R., Hayes, J. M., et al. (2005). An evaluation of ¹⁴C age relationships between co-occurring foraminifera, alkenones, and total organic carbon in continental margin sediments. *Paleoceanography* 20:A1016. doi: 10.1029/2004PA001103
- Muñiller, P. J., Kirst, G., Ruhland, G., Storch, I. V., and Rosell-Melé, A. (1998). Calibration of the alkenone paleotemperature index U_{37K'} based on core-tops from the eastern South Atlantic and the global ocean (60°N–60°S). *Geochim. Cosmochim. Acta* 62, 1757–1772.
- Narciso, Á., Gallo, F., Valente, A., Cachão, M., Cros, L., Azevedo, E. B., et al. (2016). Seasonal and interannual variations in coccolithophore abundance off Terceira Island, Azores (central north Atlantic). *Cont. Shelf Res.* 117, 43–56. doi: 10.1016/j.csr.2016.01.019
- Nürnberg, D., Bijma, J., and Hemleben, C. (1996). Assessing the reliability of magnesium in foraminiferal calcite as a proxy for water mass temperature. *Geochim. Cosmochim. Acta* 60, 803–814.
- Obata, A., Ishizaka, J., and Endoh, M. (1996). Global verification of critical depth theory for phytoplankton bloom with climatological in situ temperature and satellite ocean color data. *J. Geophys. Res.* 101, 20657–20667. doi: 10.1029/96JC01734
- Obbink, E., Carlson, A., and Klinkhammer, G. (2010). Eastern North American freshwater discharge during the Bolling-Allerod warm periods. *Geology* 38, 171–174. doi: 10.1130/g30389.1
- Ohkouchi, N., Eglinton, T., Keigwin, L., and Hayes, J. (2002). Spatial and temporal offsets between proxy records in a sediment drift. *Science* 298, 1224–1227. doi: 10.1126/science.1075287
- Osman, M., Tierney, J., Zhu, J., Tardif, R., Hakim, G., King, J., et al. (2021). Globally resolved surface temperatures since the last glacial maximum. *Nature* 599, 239–244. doi: 10.1038/s41586-021-03984-4
- Ottens, J. (1991). Planktic foraminifera as North Atlantic water mass indicators. *Oceanol. Acta* 14, 123–140. doi: 10.1371/journal.pone.0239373
- Ottens, J., and Nederbragt, A. (1992). Planktic foraminiferal diversity as indicator of ocean environments. *Mar. Micropaleontol.* 19, 13–28.
- Peck, V., Hall, I., Zahn, R., and Elderfield, H. (2008). Millennial-scale surface and subsurface paleothermometry from the northeast Atlantic, 55–8 ka BP. *Paleoceanography* 23:A3221. doi: 10.1029/2008pa001631
- Pérez-Folgado, M., Sierro, F., Flores, J., Cacho, I., Grimalt, J., Zahn, R., et al. (2003). Western Mediterranean planktonic foraminifera events and millennial climatic variability during the last 70 kyr. *Mar. Micropaleontol.* 48, 49–70. doi: 10.1016/S0377-8398(02)00160-3
- Pflaumann, U., Duprat, J., Pujol, C., and Labeyrie, L. (1996). SIMMAX: A modern analog technique to deduce Atlantic sea surface temperatures from planktonic foraminifera in deep-sea sediments. *Paleoceanography* 11, 15–35. doi: 10.1029/95pa01743
- Poulton, A. J., Holligan, P. M., Charalampopoulou, A., and Adey, T. R. (2017). Coccolithophore ecology in the tropical and subtropical Atlantic ocean: New perspectives from the Atlantic meridional transect (AMT) programme. *Prog. Oceanogr.* 158, 150–170. doi: 10.1016/j.pocean.2017.01.003
- Prahl, F. G., and Wakeham, S. G. (1987). Calibration of unsaturation patterns in long-chain ketone compositions for palaeotemperature assessment. *Nature* 330:367. doi: 10.1038/330367a0
- Raitzsch, M., Bijma, J., Benthien, A., Richter, K.-U., Steinhöfel, G., and Kucera, M. (2018). Boron isotope-based seasonal paleo-pH reconstruction for the southeast Atlantic—A multispecies approach using habitat preference of planktonic foraminifera. *Earth Planet. Sci. Lett.* 487, 138–150. doi: 10.1016/j.epsl.2018.02.002
- Rasmussen, S. O., Andersen, K. K., Svensson, A. M., Steffensen, J. P., Vinther, B. M., Clausen, H. B., et al. (2006). A new Greenland ice core chronology for the last glacial termination. *J. Geophys. Res.* 111:D06102. doi: 10.1029/2005JD006079
- Rebotim, A., Voelker, A. H. L., Jonkers, L., Waniek, J. J., Schulz, M., and Kucera, M. (2019). Calcification depth of deep-dwelling planktonic foraminifera from the eastern North Atlantic constrained by stable oxygen isotope ratios of shells from stratified plankton tows. *J. Micropaleontol.* 38, 113–131. doi: 10.5194/jm-38-113-2019
- Rebotim, A., Voelker, A. H., Jonkers, L., Waniek, J. J., Meggers, H., Schiebel, R., et al. (2017). Factors controlling the depth habitat of planktonic foraminifera in the subtropical eastern North Atlantic. *Biogeosciences* 14, 827–859. doi: 10.5194/bg-14-827-2017
- Regenberg, M., Nürnberg, D., Schönfeld, J., and Reichert, G.-J. (2007). Early diagenetic overprint in Caribbean sediment cores and its effect on the geochemical composition of planktonic foraminifera. *Biogeosciences* 4, 957–973. doi: 10.5194/bg-4-957-2007
- Regenberg, M., Steph, S., Nürnberg, D., Tiedemann, R., and Garbe-Schönberg, D. (2009). Calibrating Mg/Ca ratios of multiple planktonic foraminiferal species with $\delta^{18}\text{O}$ -calcification temperatures: Paleothermometry for the upper water column. *Earth Planet. Sci. Lett.* 278, 324–336. doi: 10.1016/j.epsl.2008.12.019
- Repschläger, J., Garbe-Schönberg, D., Weinelt, M., and Schneider, R. (2017). Holocene evolution of the North Atlantic subsurface transport. *Clim. Past* 13, 333–344. doi: 10.5194/cp-13-333-2017
- Repschläger, J., Weinelt, M., Kinkel, H., Andersen, N., Garbe-Schönberg, D., and Schwab, C. (2015). Response of the subtropical North Atlantic surface hydrography on deglacial and Holocene AMOC changes. *Paleoceanography* 30, 456–476. doi: 10.1002/2014pa002637
- Richter, T. (1998). Sedimentary fluxes at the mid-atlantic ridge—sediment sources, accumulation rates, and geochemical characterisation. *GEOMAR Rep.* 73:173.
- Rogerson, M., Rohling, E. J., Weaver, P. P. E., and Murray, J. W. (2004). The azores front since the last glacial maximum. *Earth Planet. Sci. Lett.* 222, 779–789. doi: 10.1016/j.epsl.2004.03.039
- Sabbatini, A., Bassinot, F., Boussetta, S., Negri, A., Rebaubier, H., Dewilde, F., et al. (2011). Further constraints on the diagenetic influences and salinity effect on *Globigerinoides ruber* (white) Mg/Ca thermometry: Implications in the Mediterranean Sea. *Geochem. Geophys. Geosyst.* 12:Q10005. doi: 10.1029/2011gc003675
- Salmon, K. H., Anand, P., Sexton, P. F., and Conte, M. (2015). Upper ocean mixing controls the seasonality of planktonic foraminifer fluxes and associated strength of the carbonate pump in the oligotrophic North Atlantic. *Biogeosciences* 12, 223–235. doi: 10.5194/bg-12-223-2015
- Sarnthein, M., Balmer, S., Grootes, P. M., and Mudelsee, M. (2015). Planktic and benthic ¹⁴C reservoir ages for three ocean basins, calibrated by a suite of ¹⁴C plateaus in the glacial-to-deglacial suetsu atmospheric ¹⁴C record. *Radiocarbon* 57, 129–151. doi: 10.2478/azu_rc.57.17916
- Schiebel, R. (2002). Planktic foraminiferal sedimentation and the marine calcite budget. *Glob. Biogeochem. Cycles* 16:1065. doi: 10.1029/2001GB001459
- Schiebel, R., and Hemleben, H. (2000). Interannual variability of planktic foraminiferal populations and test flux in the eastern north Atlantic ocean (JGOFS). *Deep Sea Res. Part II* 47, 1809–1852.
- Schiebel, R., and Hemleben, H. (2017). *Planktic foraminifers in the modern ocean*. Berlin: Springer-Verlag Berlin Heidelberg.
- Schiebel, R., Bijma, J., and Hemleben, C. (1997). Population dynamics of planktic foraminifer *Globigerina bulloides* from the eastern North Atlantic. *Deep Sea Res.* 44, 1701–1713.
- Schiebel, R., Brupbacher, U., Schmidtko, S., Nausch, G., Waniek, J. J., and Thierstein, H.-R. (2011). Spring coccolithophore production and dispersion in the temperate eastern north Atlantic ocean. *J. Geophys. Res.* 116:C08030. doi: 10.1029/2010jc006841
- Schiebel, R., Hiller, B., and Hemleben, C. (1995). Impacts of storms on recent planktic foraminiferal test production and CaCO₃ flux in the north Atlantic at 47°N, 20°W (JGOFS). *Mar. Micropaleontol.* 26, 115–129. doi: 10.1016/0377-8398(95)00035-6
- Schiebel, R., Schmuker, B., Alves, M., and Hemleben, C. (2002a). Tracking the recent and late pleistocene azores front by the distribution of planktic foraminifers. *J. Mar. Syst.* 37, 213–227.
- Schiebel, R., Waniek, J., Bork, M., and Hemleben, C. (2001). Planktic foraminifer production stimulated by chlorophyll redistribution and entrainment of nutrients. *Deep Sea Res. Part I* 48, 721–740. doi:10.1016/S0967-0637(00)0065-0
- Schiebel, R., Waniek, J., Zeltner, A., and Alves, M. (2002b). Impact of the Azores front on the distribution of planktic foraminifers, shelled gastropods, and coccolithophorids. *Deep Sea Res. Part II* 49, 4035–4050.
- Schlitzer, R. (2012). *Ocean data view*. Version 5.3.0. Available online at: <http://odv.awi.de>
- Schneider, B., Leduc, G., and Park, W. (2010). Disentangling seasonal signals in holocene climate trends by satellite-model-proxy integration. *Paleoceanography* 25:A4217. doi: 10.1029/2009pa001893
- Schwab, C. (2013). *Late quaternary changes in paleoproductivity and hydrography in the azores region deduced from coccolithophore assemblages*. Eldiss. Kiel: University Kiel.
- Schwab, C., Kinkel, H., Weinelt, M., and Repschläger, J. (2012). Coccolithophore paleoproductivity and ecology response to deglacial and holocene changes in the azores current system. *Paleoceanography* 27:A3210. doi:10.1029/2012pa002281
- Schwab, C., Kinkel, H., Weinelt, M., and Repschläger, J. (2013). A coccolithophore based view on paleoenvironmental changes in the open ocean mid-latitude north

- Atlantic between 130 and 48 ka BP with special emphasis on MIS 5e. *Quat. Sci. Rev.* 81, 35–47. doi: 10.1016/j.quascirev.2013.09.021
- Shackleton, N. (1974). Attainment of isotopic equilibrium ocean water and the benthonic foraminifera genus *Uvigerina*: Isotopic changes in the ocean during the last glacial. *Cent. Natl. Rech. Sci. Colloq. Int.* 219, 203–209.
- Siccha, M., and Kucera, M. (2017). ForCenS, a curated database of planktonic foraminifera census counts in marine surface sediment samples. *Sci. Data* 4:170109. doi: 10.1038/sdata.2017.109
- Sicre, M.-A., Siani, G., Genty, D., Kallel, N., and Essallami, L. (2013). Seemingly divergent sea surface temperature proxy records in the central Mediterranean during the last deglacial. *Clim. Past Discuss.* 9, 683–701. doi: 10.5194/cpd-9-683-2013
- Sikes, E., and Keigwin, L. (1996). A reexamination of northeast Atlantic sea surface temperature and salinity over the last 16 kyr. *Paleoceanography* 11, 327–342. doi: 10.1029/95pa03697
- Simstich, J., Sarnthein, M., and Erlenkeuser, H. (2003). Paired $\delta^{18}\text{O}$ signals of *Neogloboquadrina pachyderma* (s) and *Turborotalita quinqueloba* show thermal stratification structure in Nordic Seas. *Mar. Micropaleontol.* 48, 107–125. doi: 10.1016/S0377-8398(02)00165-2
- Skinner, L., and Elderfield, H. (2005). Constraining ecological and biological bias in planktonic foraminiferal Mg/Ca and $\text{d}^{18}\text{O}_{\text{cc}}$: A multispecies approach to proxy calibration testing. *Paleoceanography* 20:A1015. doi: 10.1029/2004PA001058
- Steinke, S., Kienast, M., Groeneveld, J., Lin, L., Chen, M., and Rendle-Bühning, R. (2008). Proxy dependence of the temporal pattern of deglacial warming in the tropical south China sea: Toward resolving seasonality. *Quat. Sci. Rev.* 27, 688–700.
- Storz, D., Schulz, H., Waniek, J., Schulz-Bull, D., and Kucera, M. (2009). Seasonal and interannual variability of the planktic foraminiferal flux in the vicinity of the Azores current. *Deep Sea Res. Part I* 56, 107–124. doi: 10.1016/j.dsr.2008.08.009
- Stouffer, R. J., Yin, J., Gregory, J., Dixon, K., Spelman, M., Hurlin, W., et al. (2006). Investigating the causes of the response of the thermohaline circulation to past and future climate changes. *J. Clim.* 19, 1365–1387. doi: 10.1175/JCLI13689.1
- Telford, R. J., Li, C., and Kucera, M. (2013). Mismatch between the depth habitat of planktonic foraminifera and the calibration depth of SST transfer functions may bias reconstructions. *Clim. Past* 9, 859–870. doi: 10.5194/cp-9-859-2013
- Teller, J. T., Leverington, D. W., and Mann, J. D. (2002). Freshwater outbursts to the oceans from glacial Lake Agassiz and their role in climate change during the last deglaciation. *Quat. Sci. Rev.* 21, 879–887. doi: 10.1016/S0277-3791(01)00145-7
- Thornalley, D. J. R., Elderfield, H., and McCave, I. N. (2011). Reconstructing North Atlantic deglacial surface hydrography and its link to the Atlantic overturning circulation. *Glob. Planet. Change* 79, 163–175. doi: 10.1016/j.gloplacha.2010.06.003
- Thornalley, D. J. R., McCave, I. N., and Elderfield, H. (2010). Freshwater input and abrupt deglacial climate change in the North Atlantic. *Paleoceanography* 25:A1201. doi: 10.1029/2009PA001772
- Waelbroeck, C., Labeyrie, L. D., Michel, E., Duplessy, J. C., McManus, J. F., Lambeck, K., et al. (2002). Sea-level and deep water temperature changes derived from benthic foraminifera isotopic records. *Quat. Sci. Rev.* 21, 295–305.
- Weinelt, M., Schwab, C., Kneisel, J., and Hinz, M. (2015). “Climate and societal change in the western Mediterranean area around 4.2 ka BP” in *2200 BC—Ein klimasturz als ursache für den zerfall der alten welt? 2200 BC—A climatic breakdown as a cause for the collapse of the old world? 7. Mitteldeutscher archäologentag vom 17. bis 19. Oktober 2013 in Halle (Saale). 7th archaeological conference of central Germany october 23–26, 2014 in Halle (Saale)*, Vol. 1, eds H. Meller, H. Arz, R. Jung, and R. Risch (Halle (Saale): Tagungen des Landesmuseums für Vorgeschichte Halle), 461–480.
- Wilke, I., Meggers, H., and Bickert, T. (2009). Depth habitats and seasonal distributions of recent planktic foraminifers in the Canary Islands region (29°N) based on oxygen isotopes. *Deep Sea Res. Part I* 56, 89–106. doi: 10.1016/j.dsr.2008.08.001
- Wolfeich, C. M. (1994). *Satellite-derived sea surface temperature, mesoscale variability, and foraminiferal production in the North Atlantic*. Ph.D. thesis. Falmouth: MIT and WHOI.
- Yamasaki, M., Tokumoto, R., Sasaki, A., Shimada, C., and Schiebel, R. (2022). Western to central equatorial pacific planktic foraminiferal fluxes: Implication for the relationship between their assemblage and warm pool migration from 1999 to 2002. *J. Foraminifer. Res.* 52, 140–159. doi: 10.2113/gsjfr.52.3.140